frontiers in Plant Science

ORIGINAL RESEARCH
published: 18 January 2021
doi: 10.3389/fpls.2020.613499

Etiology of *Cyclocarya paliurus* Anthracnose in Jiangsu Province, China

*Xiang-rong Zheng, Mao-jiao Zhang, Xu-lan Shang, Sheng-zuo Fang and Feng-mao Chen**

Collaborative Innovation Center of Sustainable Forestry in Southern China, College of Forestry, Nanjing Forestry University, Nanjing, China

Cyclocarya paliurus is an extremely valuable and multifunctional tree species whose leaves have traditionally been used in used in medicine or as a medicinal tea in China. In recent years, anthracnose has been frequently observed on young leaves of *C. paliurus* in several nurseries located in Jiangsu Province, resulting in great yield and quality losses. To date, no information is available about the prevalence of *C. paliurus* anthracnose in China. The main purpose of the present study was to characterize the etiology of *C. paliurus* anthracnose. Phylogenetic analysis of the eight-loci concatenated dataset revealed that all 44 single-spore *Colletotrichum* isolates belonged to three species in the *Colletotrichum gloeosporioides* species complex, namely, *Colletotrichum aenigma*, *Colletotrichum fructicola*, and *C. gloeosporioides* sensu stricto. Phenotypic features, including the colony appearance and the morphology of conidia, appressoria, and ascospores, were consistent with the phylogenetic grouping. Virulence tests validated that the three *Colletotrichum* species could cause typical symptoms of anthracnose on *C. paliurus* leaves, similar to those observed in the field. The optimum mycelial growth temperature ranged from 25 to 30°C for all representative isolates, while *C. gloeosporioides* s. s. isolates exhibited greater tolerance to high temperature (40°C). Fungicide sensitivity assays indicated that all three *Colletotrichum* species were sensitive to tetramycin, which may be a potential alternative for the management of *C. paliurus* anthracnose. To our knowledge, this study provides the first report of *C. aenigma*, *C. fructicola*, and *C. gloeosporioides* s. s. causing *C. paliurus* anthracnose in China as well as in the world.

Keywords: *Cyclocarya paliurus*, etiology, fungicide sensitivity, *Colletotrichum*, anthracnose

OPEN ACCESS

Edited by:
Sajeewa S. N. Maharachchikumbura, University of Electronic Science and Technology of China, China

Reviewed by:
Gunjan Sharma, Agricultural Research Organization (ARO), Israel
Ruvishika Jayawardena, Mae Fah Luang University, Thailand

****Correspondence:***
Feng-mao Chen
cfengmao@njfu.edu.cn

Specialty section:
This article was submitted to Plant Pathogen Interactions, a section of the journal Frontiers in Plant Science

Received: *02 October 2020*
Accepted: *28 December 2020*
Published: *18 January 2021*

Citation:
Zheng X-r, Zhang M-j, Shang X-l, Fang S-z and Chen F-m (2021) Etiology of Cyclocarya paliurus Anthracnose in Jiangsu Province, China. Front. Plant Sci. 11:613499. doi: 10.3389/fpls.2020.613499

INTRODUCTION

Cultivated for fine timber and as a medicinal plant, *Cyclocarya paliurus* is the sole extant species in the genus *Cyclocarya* and is native to China, naturally distributed in mountainous regions in the middle and lower reaches of the Yangtze River (Fang et al., 2011; Deng et al., 2015; Xie et al., 2015; Zheng et al., 2020). In Chinese folklore, *C. paliurus* is commonly called the "sweet tea tree,"

and its leaves have traditionally been used as drug formulations for the treatment of obesity or diabetes mellitus (Fang et al., 2011; Cao et al., 2017; Xie et al., 2018). In recent years, increasing attention has been paid to *C. paliurus* because phytochemical studies have demonstrated that the extracts of its leaves possess a wide range of biological activities beneficial to human beings, such as antihypertensive (Xie et al., 2006), hypoglycemic (Wang et al., 2013), anti-HIV-1 (Zhang et al., 2010), antioxidant (Xie et al., 2010; Wang et al., 2013; Liu et al., 2018a,b), antitumor (Liu et al., 2018b), and anticancer (Xie et al., 2013) activities. Current focal studies of *C. paliurus* have concentrated on producing or identifying the bioactive components in its leaves. Unfortunately, to date, no information about *C. paliurus* anthracnose is available, and this disease could become a limiting factor affecting the *C. paliurus* tea industry.

The Coelomycetous genus *Colletotrichum* Corda includes plant pathogens responsible for anthracnose diseases with a global distribution (Hyde et al., 2009; Wikee et al., 2011; Cannon et al., 2012; Dean et al., 2012; He et al., 2019). From the perspective of economic and scientific importance, *Colletotrichum* was denoted the eighth most significant fungal phytopathogen group worldwide (Dean et al., 2012), attacking over 3200 dicot and monocot plant species (Manire et al., 2002; O'Connell et al., 2012). The morphological taxonomy of *Colletotrichum* species has historically been arduous owing to overlapping characteristics, and the morphology sometimes varies with environmental factors (e.g., temperature, illumination, etc.) in culture (Freeman et al., 1998; Cannon et al., 2012; Damm et al., 2019). Molecular tools have been widely applied to effectively identify and define fungi at the species level. In recent years, the majority of studies regarding anthracnose were conducted principally via morphology and multigene phylogeny based on modern taxonomic concepts, which provides a more precise and robust solution (Damm et al., 2012; Liu et al., 2014, 2015; De Silva et al., 2017a; Diao et al., 2017; Guarnaccia et al., 2017; Fu et al., 2019).

Colletotrichum spp. infections initially occur via the attachment of spores to the host plant surface, followed by spore germination and the formation of an appressorium, which penetrates the plant cuticle. This process suggests that appressoria and spores play a critical role in the infection cycle and that certain highly inhibitory substances against spore germination and appressorium production would be potential alternatives to control anthracnose (De Silva et al., 2017b; Gao et al., 2020; Konsue et al., 2020). Currently, chemical pesticides are identified as the principal agents used for anthracnose management (Bi et al., 2011). However, excessive use of such chemicals has also brought a series of challenges over time (Lu et al., 2010; Hu et al., 2015; Duan et al., 2018), including pathogen resistance and residual toxicity that affects human health and the environment (Kim et al., 2015; Alijani et al., 2019). The selection of environmentally safe, high-efficacy and relatively new fungicides is therefore imperative.

The application of antibiotic fungicides derived from metabolites of beneficial microbes to control phytopathogens has recently attracted increased attention since these compounds have been found to be environmentally friendly and may help to overcome pesticide resistance due to their low toxicity to non-target organisms and structural versatility (Moreira and May De Mio, 2015; Simionato et al., 2017; Han et al., 2020), offering a safe and effective way to circumvent the drawbacks of chemically synthesized pesticides and decreasing the environmental risks associated with their contamination (Ma et al., 2018a; Zhu et al., 2018).

Tetramycin, the fermentation metabolite of *Streptomyces ahygroscopicus*, exhibits excellent inhibitory activity against many plant pathogens, including *Botrytis cinera*, *Passalora fulva*, *Phytophthora capsici*, and *Pyricularia oryzae* (Zhong et al., 2010; Ren et al., 2014; Song et al., 2016; Chen L. L. et al., 2017; Ma et al., 2018a), which has been registered to manage rice and fruit crop diseases in China (Zhao et al., 2010). On the other hand, a previous study reported that tetramycin has the potential to elicit disease resistance by activating plant defensive enzymes, including polyphenol oxidase (PPO), peroxidase (POD), and phenylalanine ammonia lyase (PAL) (Zhong et al., 2010). Owing to its environmental friendliness and high efficiency, tetramycin has become the preferred fungicide in recent years (Song et al., 2016; Ma et al., 2018a,b).

Phenazine-1-carboxylic acid (PCA) is an important N-containing heterocyclic secondary metabolite (Zhu et al., 2019), which has been proved having antimicrobial (Palchykovska et al., 2012; Udumula et al., 2017), antitumorigenic (Gupta et al., 2014), antiviral, and antitubercular effects (Logua et al., 2009; Palchykovska et al., 2012), widely existed in microbial metabolites of *Pseudomonads* and *Streptomycetes* (Zhu et al., 2019). Particularly, in recent years, PCA received much attention due to outstanding inhibition effects against several phytopathogenic fungi in agricultural application (Zhu et al., 2019; Han et al., 2020). In China, PCA has been registered as the biofungicide "Shenqinbactin" for its environmental friendliness, low toxicity to human and animals, and the enhancement of crop production (Zhu et al., 2018, 2019; Han et al., 2020).

Kasugamycin, the fermentation product of *Streptomyces kasugaensis*, is a member of the aminoglycoside antibiotic (Uppala and Zhou, 2018). It was originally developed as a biofungicide for the management of rice blast caused by *P. oryzae*. Kasugamycin inhibits protein biosynthesis, with both fungicidal and bactericidal activities (McGhee and Sundin, 2011). Due to it is high efficiency and friendliness to environment, the use of Kasugamycin in United States has been approved by EPA for controlling diseases of several pome fruits in the past decade[1].

In 2018, during an investigation of *C. paliurus*, serious anthracnose symptoms (**Figure 1A**) were observed in several nurseries located in the scientific research base of Nanjing Forestry University in Baima town (Baima), Nanjing. Over a half of the leaves were infected in Baima based on our observation. This anthracnose has been considered an emerging disease, but it is becoming endemic; nevertheless, the etiology, epidemiology, and management of this disease are uncertain. Hence, the objectives of the present study were to (1) accurately identify the *Colletotrichum* spp. causing

[1]https://www.federalregister.gov/documents/2014/08/29/2014-20502/kasugamycin-pesticide-tolerances

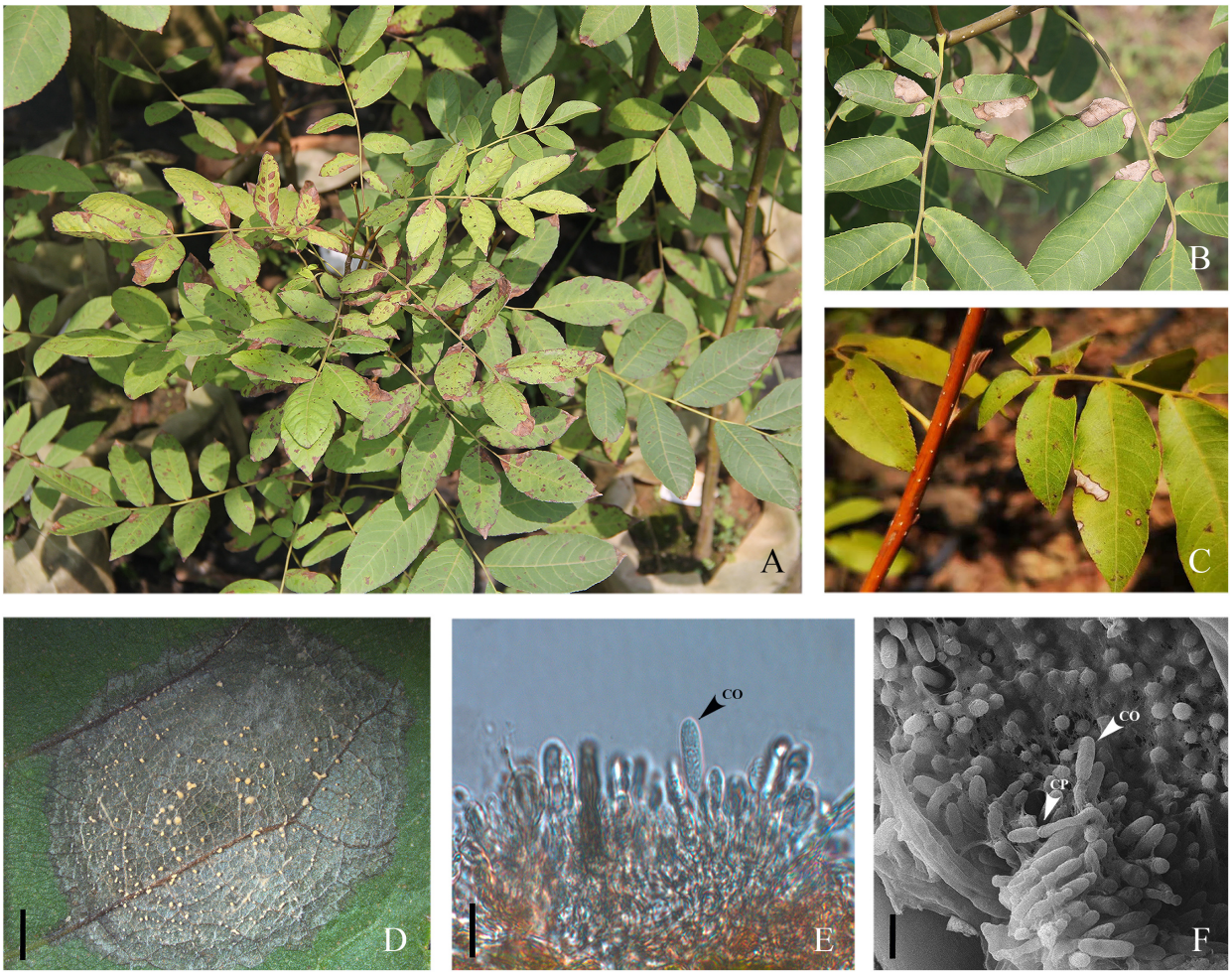

FIGURE 1 | *Cyclocarya paliurus* leaves with typical necrosis symptoms of anthracnose. **(A)** Diseased leaves in the field. **(B,C)** Initial and later symptoms of *Cyclocarya paliurus* anthracnose. **(D)** Gelatinous orange spore masses oozed and arranged in concentric rings; bar = 2 mm. **(E)** Longitudinal section of acervuli developed on leaf lesion; co indicates conidia; bar = 10 μm. **(F)** Scanning electron photomicrograph of acervuli formed on leaf lesion; co and cp indicate conidia and conidiophores, respectively; bar = 10 μm.

C. paliurus anthracnose in Jiangsu Province, China, combining morphological and biological characteristics with molecular phylogenetic analyses; (2) examine the virulence of these fungi on *C. paliurus* leaves *in vitro*; and (3) characterize and compare the inhibitory effects of biofungicides against different *Colletotrichum* spp. *in vitro*.

MATERIALS AND METHODS

Field Survey and Sampling

A field survey of *C. paliurus* anthracnose was carried out in Nanjing (five nurseries), Changzhou (four nurseries), and Yancheng (four nurseries) in September and October 2018 during the late growing season. Disease incidence was calculated as the percentage of trees displaying anthracnose symptoms out of the total number of evaluated trees (Bautista-Cruz et al., 2019). Three leaves exhibiting typical symptoms of anthracnose were randomly sampled per plant, and at least 10 symptomatic plants were sampled per nursery. All samples were then packaged in self-sealing bags and transported in an ice chest to the laboratory and then stored at 5°C prior to isolation.

Colletotrichum Isolation

To isolate the fungus, small sections (4-by-4 mm pieces) were removed from the margin of leaf lesions, surface disinfected in 1% (vol/vol) $NaClO_3$ for 45 s and 75% ethanol for 30 s, rinsed in sterile distilled water three times, and air-dried on sterilized paper. The sections were then cultured onto 2% potato dextrose agar (PDA) (five sections per plate) amended with 100 μg/mL ampicillin to inhibit bacterial growth and incubated at 25°C in the dark. The emerging edges of the fungal mycelium were observed daily and transferred aseptically onto new PDA plates. Colonies similar in morphology to *Colletotrichum* spp. were purified using the monosporic isolation procedure described by Cai et al. (2009), and single-spore cultures were preserved in

PDA slant test tubes at 4°C for follow-up studies. All isolates used in this study were deposit in State Key Laboratory of Forest Protection in Nanjing Forestry University.

Molecular Identification and Phylogenetic Analysis

For further characterization of the *Colletotrichum* spp., total genomic DNA (gDNA) of all single-spore isolates was extracted following the CTAB method described by Than et al. (2008). The concentrations of gDNA extracts were adjusted to 100 ng/μL with autoclaved double distilled water (ddH_2O) using a NanoDrop 2000 spectrophotometer (Thermo Fisher Scientific, Madison, WI, United States) and stored at −20°C before use. Polymerase chain reaction (PCR) amplification was performed for the following loci: the ITS region, calmodulin (CAL), β-tubulin (TUB), actin (ACT), chitin synthase 1 (CHS-1), glyceraldehyde-3-phosphate dehydrogenase (GAPDH), glutamine synthetase (GS), and Apn2-Mat1-2 intergenic spacer (ApMat) genes. PCR amplifications were conducted in a 25 μL volume, mixed with 8.5 μL of ddH_2O, 1 μL of each primer (10 μM), 2 μL of template DNA, and 12.5 μL of 2 × PCR Taq Master Mix (Applied Biological Materials Inc., Canada), using an Eppendorf Nexus Thermal Cycler (Germany). A negative control was added in all amplifications, where an equal volume of ddH_2O replaced the template DNA. The primers and PCR settings for each locus are shown in **Table 1**. Amplification products were purified and sequenced by Jie Li Biotech Company (Shanghai, China). Forward and reverse DNA sequences were assembled and manually edited where necessary using Bioedit software (version 7.0.5[2]), and the consensus sequences were deposited in GenBank (**Table 2**). Reference sequences from ex-type or other authoritative specimens of *Colletotrichum* spp. were retrieved from GenBank and aligned with sequences generated herein for constructing phylogenetic trees, with *C. boninense* (MAFF 305972) used as an outgroup (**Tables 2**, **3**).

The phylogenetic analysis for each individual locus and the concatenated matrix were inferred under the Bayesian inference (BI) and maximum-likelihood (ML) criteria in MrBayes 3.2.6 (Ronquist et al., 2012) and MEGA 7 (Kumar et al., 2016), respectively. For BI analysis, the best nucleotide substitution model of each locus was ascertained by MrModeltest 2.3 according to AICc, with K2 + I identified for CHS, TN93 identified for GADPH, K2 + G identified for ACT and ApMat, GTR + G identified for CAL and GS, and TN93 + G identified for ITS and TUB. Four Markov chains were run for 30 million generations simultaneously, with trees sampled every 1000 generations. The first 25% of trees were discarded as the burn-in phase of the analyses, while the remaining trees were used for calculating posterior probabilities (PPs) in the majority rule consensus tree. ML analysis was performed based on the GTR + G + I model, and clade support was determined by 1000 bootstrap replicates, with gaps treated as missing data.

Morphological and Biological Characterization

Fourteen representative isolates were selected for further studies according to BI/ML phylogenetic analysis (**Table 1**). Mycelial blocks (2 mm in side length) aseptically taken from actively growing cultures were transferred to new PDA plates and incubated at 25°C in darkness. Colony characteristics, including conidiomata or ascomata production, were determined up to 30 days post-inoculation (dpi). Conidia, appressoria, ascospores, and asci for microscopy were obtained and examined according to the procedure described by Weir et al. (2012). At least 30 measurements per structure were recorded at ×100 magnification using a ZEISS Axio Imager A2m microscope (Carl Zeiss, Göttingen, Germany) equipped with differential interference contrast (DIC) optics. To observe fungal structures developed on infected tissue, leaves showing typical symptoms of anthracnose were collected and prepared using the method of Huang et al. (2018), with photomicrographs taken by a Regulus 8100 field emission scanning electron microscope (FE-SEM, Japan).

To determine the optimal temperature for colony growth, mycelial blocks (2 mm in side length) of 14 representative isolates were cultured as described above and incubated at temperatures of 5–40°C with 5°C intervals. The colony diameter was measured at two perpendicular angles, and the average was taken at 4 dpi. Five replicates per isolate were examined at all eight temperatures, and the experiment was conducted twice. Differences in the morphological and biological characteristics of the isolates were determined by one-way analysis of variance (ANOVA) using IBM SPSS Statistics 24.0 software (SPSS, Inc., Chicago, IL, United States).

Virulence Tests of *Colletotrichum* Isolates

Virulence tests were conducted with reference to previous reports with minor modifications (Huang et al., 2016; Chen Y. et al., 2017; Xue et al., 2019). Fourteen representative *Colletotrichum* isolates were selected and cultured on PDA and used for virulence tests on detached *C. paliurus* leaves under controlled conditions (**Table 2**). Conidial suspensions of each isolate were prepared as previously described and adjusted to two concentrations of 1×10^6 and 1×10^8 conidia/mL with ddH_2O.

Asymptomatic *C. paliurus* leaves were surface disinfected and air-dried as mentioned above, and then one piercing wound was made on the right side of each leaf using a sterile needle (insect pin, 0.71 mm in diameter), or the leaves were left unwounded. Wound inoculation was performed by placing an 8 μL conidial suspension (1×10^6 conidia/mL) or mycelial blocks (5 mm in length) from margins of actively growing colonies onto each stab wound. Non-wound inoculation was conducted by placing an 8 μL spore suspension (1×10^8 conidia/mL) or mycelial blocks onto the mid-right region of the leaves without pin pricking. Leaves inoculated with ddH_2O or non-colonized PDA blocks were treated as negative controls. The experiment was conducted in triplicate for each treatment and control, involving five leaves per replicate. All treatments and controls were placed into transparent containers (334 × 215 × 87 mm) lined with moist sterile filter paper and sealed by plastic wrap to maintain a high relative humidity and then incubated at 25°C under a 12 h photoperiod in a growth chamber. The whole experiment was carried out twice.

[2]http://www.mbio.ncsu.edu/bioedit/page2.html

TABLE 1 | Descriptions and sequence accession numbers obtained from GenBank of the *Colletotrichum* spp. used in the phylogenetic study.

Species	Culture/Isolate[a]	Host	City/Country	GenBank accession number[b]							
				ITS	GAPDH	CAL	ACT	CHS-1	TUB	GS	ApMat
C. aenigma	**ICMP 18608**	*Persea americana*	Israel	JX010244	JX010044	JX009683	JX009443	JX009774	JX010389	JX010078	KM360143
	HC3[c]	*Cyclocarya paliurus*	Changzhou, China	*MT476807*	*MT501007*	*MT500919*	*MT500875*	*MT500963*	*MT501051*	*MW344671*	*MW344720*
	JS2	*C. paliurus*	Changzhou, China	*MT476808*	*MT501008*	*MT500920*	*MT500876*	*MT500964*	*MT501052*	*MW344672*	*MW344721*
	JS7	*C. paliurus*	Changzhou, China	*MT476809*	*MT501009*	*MT500921*	*MT500877*	*MT500965*	*MT501053*	*MW344673*	*MW344722*
	SC7[c]	*C. paliurus*	Nanjing, China	*MT476810*	*MT501010*	*MT500922*	*MT500878*	*MT500966*	*MT501054*	*MW344674*	*MW344723*
	YM8[c]	*C. paliurus*	Yancheng, China	*MT476811*	*MT501011*	*MT500923*	*MT500879*	*MT500967*	*MT501055*	*MW344675*	*MW344724*
	ZH2	*C. paliurus*	Yancheng, China	*MT476812*	*MT501012*	*MT500924*	*MT500880*	*MT500968*	*MT501056*	*MW344676*	*MW344725*
C. aeschynomenes	**ICMP 17673**	*Aeschynomene virginica*	United States	JX010176	JX009930	JX009721	JX009483	JX009799	JX010392	JX010081	KM360145
C. alatae	**CBS 304.67**, ICMP 17919	*Dioscorea alata*	India	JX010190	JX009990	JX009738	JX009471	JX009837	JX010383	JX010065	KC888932
C. alienum	**ICMP 12071**	*Malus domestica*	New Zealand	JX010251	JX010028	JX009654	JX009572	JX009882	JX010411	JX010101	KM360144
C. aotearoa	**ICMP 18537**	*Coprosma* sp.	New Zealand	JX010205	JX010005	JX009611	JX009564	JX009853	JX010420	JX010113	KC888930
C. arecicola	CGMCC 3.19667, **HNBL5**	*Areca catechu*	Wenchang, China	MK914635	MK935455		MK935374	MK935541	MK935498		MK935413
C. asianum	**ICMP 18580**, CBS 130418	*Coffea arabica*	Thailand	FJ972612	JX010053	FJ917506	JX009584	JX009867	JX010406	JX010096	FR718814
C. boninense	**MAFF 305972**	*Crinum asiaticum var. sinicum*	Japan	JX010292	JX009905	JQ005674	JX009583	JX009827	JQ005588		
C. clidemiae	**ICMP 18658**	*Clidemia hirta*	United States, Hawaii	JX010265	JX009989	JX009645	JX009537	JX009877	JX010438	JX010129	KC888929
C. cordylinicola	**MFLUCC 090551**, ICMP 18579	*Cordyline fruticosa*	Thailand	JX010226	JX009975	HM470238	HM470235	JX009864	JX010440	JX010122	JQ899274
C. fructicola	**ICMP 18581**, CBS 130416	*Coffea arabica*	Thailand	JX010165	JX010033	FJ917508	FJ907426	JX009866	JX010405	JX010095	JQ807838
	BM5[c]	*C. paliurus*	Nanjing, China	*MT476813*	*MT501013*	*MT500925*	*MT500881*	*MT500969*	*MT501057*	*MW344677*	*MW344726*
	BX1	*C. paliurus*	Nanjing, China	*MT476814*	*MT501014*	*MT500926*	*MT500882*	*MT500970*	*MT501058*	*MW344678*	*MW344727*
	F5	*C. paliurus*	Changzhou, China	*MT476815*	*MT501015*	*MT500927*	*MT500883*	*MT500971*	*MT501059*	*MW344679*	*MW344728*
	GX1[c]	*C. paliurus*	Changzhou, China	*MT476816*	*MT501016*	*MT500928*	*MT500884*	*MT500972*	*MT501060*	*MW344680*	*MW344729*
	GT7	*C. paliurus*	Changzhou, China	*MT476817*	*MT501017*	*MT500929*	*MT500885*	*MT500973*	*MT501061*	*MW344681*	*MW344730*
	HC2[c]	*C. paliurus*	Changzhou, China	*MT476818*	*MT501018*	*MT500930*	*MT500886*	*MT500974*	*MT501062*	*MW344682*	*MW344731*
	HC6	*C. paliurus*	Changzhou, China	*MT476819*	*MT501019*	*MT500931*	*MT500887*	*MT500975*	*MT501063*	*MW344683*	*MW344732*
	JS3	*C. paliurus*	Changzhou, China	*MT476820*	*MT501020*	*MT500932*	*MT500888*	*MT500976*	*MT501064*	*MW344684*	*MW344733*
	JS9	*C. paliurus*	Changzhou, China	*MT476821*	*MT501021*	*MT500933*	*MT500889*	*MT500977*	*MT501065*	*MW344685*	*MW344734*
	LC7[c]	*C. paliurus*	Nanjing, China	*MT476822*	*MT501022*	*MT500934*	*MT500890*	*MT500978*	*MT501066*	*MW344686*	*MW344735*
	LG2	*C. paliurus*	Nanjing, China	*MT476823*	*MT501023*	*MT500935*	*MT500891*	*MT500979*	*MT501067*	*MW344687*	*MW344736*
	LG4	*C. paliurus*	Nanjing, China	*MT476824*	*MT501024*	*MT500936*	*MT500892*	*MT500980*	*MT501068*	*MW344688*	*MW344737*
	LV2	*C. paliurus*	Nanjing, China	*MT476825*	*MT501025*	*MT500937*	*MT500893*	*MT500981*	*MT501069*	*MW344689*	*MW344738*
	NC25[c]	*C. paliurus*	Nanjing, China	*MT476826*	*MT501026*	*MT500938*	*MT500894*	*MT500982*	*MT501070*	*MW344690*	*MW344739*
	NC26	*C. paliurus*	Nanjing, China	*MT476827*	*MT501027*	*MT500939*	*MT500895*	*MT500983*	*MT501071*	*MW344691*	*MW344740*
	PL2	*C. paliurus*	Changzhou, China	*MT476828*	*MT501028*	*MT500940*	*MT500896*	*MT500984*	*MT501072*	*MW344692*	*MW344741*
	PX3	*C. paliurus*	Changzhou, China	*MT476829*	*MT501029*	*MT500941*	*MT500897*	*MT500985*	*MT501073*	*MW344693*	*MW344742*
	SC6[c]	*C. paliurus*	Nanjing, China	*MT476830*	*MT501030*	*MT500942*	*MT500898*	*MT500986*	*MT501074*	*MW344694*	*MW344743*
	SC9	*C. paliurus*	Nanjing, China	*MT476831*	*MT501031*	*MT500943*	*MT500899*	*MT500987*	*MT501075*	*MW344695*	*MW344744*
	T5	*C. paliurus*	Nanjing, China	*MT476832*	*MT501032*	*MT500944*	*MT500900*	*MT500988*	*MT501076*	*MW344696*	*MW344745*
	T9	*C. paliurus*	Nanjing, China	*MT476833*	*MT501033*	*MT500945*	*MT500901*	*MT500989*	*MT501077*	*MW344697*	*MW344746*
	H3	*C. paliurus*	Nanjing, China	*MT476834*	*MT501034*	*MT500946*	*MT500902*	*MT500990*	*MT501078*	*MW344698*	*MW344747*
	H4	*C. paliurus*	Nanjing, China	*MT476835*	*MT501035*	*MT500947*	*MT500903*	*MT500991*	*MT501079*	*MW344699*	*MW344748*
	YH6[c]	*C. paliurus*	Yancheng, China	*MT476836*	*MT501036*	*MT500948*	*MT500904*	*MT500992*	*MT501080*	*MW344700*	*MW344749*

(Continued)

TABLE 1 | Continued

Species	Culture/Isolate[a]	Host	City/Country	GenBank accession number[b]							
				ITS	GAPDH	CAL	ACT	CHS-1	TUB	GS	ApMat
	YH7	*C. paliurus*	Yancheng, China	*MT476837*	*MT501037*	*MT500949*	*MT500905*	*MT500993*	*MT501081*	*MW344701*	*MW344750*
	YM2	*C. paliurus*	Yancheng, China	*MT476838*	*MT501038*	*MT500950*	*MT500906*	*MT500994*	*MT501082*	*MW344702*	*MW344751*
	YM7	*C. paliurus*	Yancheng, China	*MT476839*	*MT501039*	*MT500951*	*MT500907*	*MT500995*	*MT501083*	*MW344703*	*MW344752*
	ZH6	*C. paliurus*	Yancheng, China	*MT476840*	*MT501040*	*MT500952*	*MT500908*	*MT500996*	*MT501084*	*MW344704*	*MW344753*
C. gloeosporioides	IMI 356878, **ICMP 17821,** CBS 112999	*Citrus sinensis*	Italy	JX010152	JX010056	JX009731	JX009531	JX009818	JX010445	JX010085	JQ807843
	BM6[c]	*C. paliurus*	Nanjing, China	*MT476841*	*MT501041*	*MT500953*	*MT500909*	*MT500997*	*MT501085*	*MW344705*	*MW344754*
	F8	*C. paliurus*	Changzhou, China	*MT476842*	*MT501042*	*MT500954*	*MT500910*	*MT500998*	*MT501086*	*MW344706*	*MW344755*
	GX3[c]	*C. paliurus*	Changzhou, China	*MT476843*	*MT501043*	*MT500955*	*MT500911*	*MT500999*	*MT501087*	*MW344707*	*MW344756*
	JS1	*C. paliurus*	Changzhou, China	*MT476844*	*MT501044*	*MT500956*	*MT500912*	*MT501000*	*MT501088*	*MW344708*	*MW344757*
	JS5	*C. paliurus*	Changzhou, China	*MT476845*	*MT501045*	*MT500957*	*MT500913*	*MT501001*	*MT501089*	*MW344709*	*MW344758*
	LC2[c]	*C. paliurus*	Nanjing, China	*MT476846*	*MT501046*	*MT500958*	*MT500914*	*MT501002*	*MT501090*	*MW344710*	*MW344759*
	LC6	*C. paliurus*	Nanjing, China	*MT476847*	*MT501047*	*MT500959*	*MT500915*	*MT501003*	*MT501091*	*MW344711*	*MW344760*
	YM4[c]	*C. paliurus*	Yancheng, China	*MT476848*	*MT501048*	*MT500960*	*MT500916*	*MT501004*	*MT501092*	*MW344712*	*MW344761*
	YM5	*C. paliurus*	Yancheng, China	*MT476849*	*MT501049*	*MT500961*	*MT500917*	*MT501005*	*MT501093*	*MW344713*	*MW344762*
	ZH3	*C. paliurus*	Yancheng, China	*MT476850*	*MT501050*	*MT500962*	*MT500918*	*MT501006*	*MT501094*	*MW344714*	*MW344763*
C. horii	**NBRC 7478**, ICMP 10492	*Diospyros kaki*	Japan	*GQ329690*	*GQ329681*	*JX009604*	*JX009438*	*JX009752*	*JX010450*	JX010137	JQ807840
C. kahawae subsp. *ciggaro*	**ICMP 18539**	*Olea europaea*	Australia	JX010230	JX009966	JX009635	JX009523	JX009800	JX010434	JX010132	
C. kahawae subsp. *kahawae*	IMI 319418, **ICMP 17816**	*Coffea arabica*	Kenya	JX010231	JX010012	JX009642	JX009452	JX009813	JX010444	JX010130	JQ894579
C. ledongense	LD1683, **CGMCC 3.18888**	*Hevea brasiliensis*	Hainan, China	MG242009	MG242017	MG242013	MG242015	MG242019	MG242011	MG242021	
C. musae	**CBS 116870**, ICMP 19119	*Musa* sp.	United States	JX010146	JX010050	JX009742	JX009433	JX009896	HQ596280	JX010103	KC888926
C. noveboracense	**AFKH109**, CBS 146410	*Malus domestica*	United States	MN646685	MN640567	MN640566	MN640565		MN640569	MN640568	MN640564
C. nupharicola	**ICMP 18187,** CBS:470.96	*Nuphar lutea subsp. polysepala*	United States	JX010187	JX009972	JX009663	JX009437	JX009835	JX010398	JX010088	JX145319
C. perseae	**GA100, CBS 141365**	*Persea americana*	Israel	KX620308	KX620242	KX620206	KX620145		KX620341	KX620275	KX620177
C. psidii	**CBS 145.29,** ICMP 19120	*Psidium* sp.	Italy	JX010219	JX009967	JX009743	JX009515	JX009901	JX010443	JX010133	KC888931
C. queenslandicum	**ICMP 1778**	*Carica papaya*	Australia	JX010276	JX009934	JX009691	JX009447	JX009899	JX010414	JX010104	KC888928
C. salsolae	**ICMP 19051**	*Salsola tragus*	Hungary	JX010242	JX009916	JX009696	JX009562	JX009863	JX010403	JX010093	KC888925
C. siamense	**ICMP 18578**, CBS 130417	*Coffea arabica*	Thailand	JX010171	JX009924	FJ917505	FJ907423	JX009865	JX010404	JX010094	JQ899289
C. siamense (syn. *C. hymenocallidis*)	**CBS 125378**, ICMP 18642	*Hymenocallis americana*	China	JX010278	JX010019	JX009709	GQ856775	GQ856730	JX010410	JX010100	JQ899283
C. theobromicola	**CBS 124945**, ICMP 18649	*Theobroma cacao*	Panama	JX010294	JX010006	JX009591	JX009444	JX009869	JX010447	JX010139	KC790726
C. ti	**ICMP 4832**	*Cordyline* sp.	New Zealand	JX010269	JX009952	JX009649	JX009520	JX009898	JX010442	JX010123	KM360146
C. tropicale	**CBS 124949**, ICMP 18653	*Theobroma cacao*	Panama	JX010264	JX010007	JX009719	JX009489	JX009870	JX010407	JX010097	KC790728
C. xanthorrhoeae	**BRIP 45094**, ICMP 17903, CBS 127831	*Xanthorrhoea preissii*	Australia	JX010261	JX009927	JX009653	JX009478	JX009823	JX010448	JX010138	KC790689

[a]*Culture numbers in bold type represent ex-type or other authentic specimens.*
BRIP, Plant Pathology Herbarium, Department of Employment, Economic, Development and Innovation, Queensland, Australia; CBS, Culture collection of the Centraalbureau voor Schimmelcultures, Fungal Biodiversity Centre, Utrecht, Netherlands; ICMP, International Collection of Microorganisms from Plants, Auckland, New Zealand; IMI, Culture collection of CABI Europe UK Centre, Egham, United Kingdom; MAFF, MAFF Genebank Project, Ministry of Agriculture, Forestry and Fisheries, Tsukuba, Japan; MFLUCC, Mae Fah Luang University Culture Collection, ChiangRai, Thailand; NBRC, NITE Biological Resource Centre, Japan. MAFF 305972 (C. boninense) was added as an outgroup.
[b]*Sequences in italics were generated in this study. ITS, internal transcribed spacers 1 and 2 together with 5.8S nrDNA; GAPDH, partial glyceraldehyde-3-phosphate dehydrogenase gene; CAL, partial calmodulin gene; ACT, partial actin gene; CHS-1, partial chitin synthase 1 gene; TUB2, partial beta-tubulin gene.*
[c]*Isolates used for morphological and biological analysis, virulence tests, and biofungicide sensitivity assays.*

TABLE 2 | Primers used in this study, with sequences, conditions and sources.

Gene	Product name	Primer	Direction	Sequence (5′-3′)	PCR conditions	References
ITS	Internal transcribed spacer	ITS1	Forward	CTTGGTCATTTAGAGGAAGTAA	Denaturation for 4 min at 94°C, followed by 30 cycles; 30 s at 94°C, 30 s at 55°C, 30 s at 72°C, and a final extension of 10 min at 72°C	Gardes and Bruns, 1993
		ITS4	Reverse	TCCTCCGCTTATTGATATGC		White et al., 1990
GAPDH	Glyceraldehyde-3-phosphate dehydrogenase	GDF1	Forward	GCCGTCAACGACCCCTTCATTGA	Denaturation for 4 min at 94°C, followed by 30 cycles; 30 s at 94°C, 30 s at 60°C, 30 s at 72°C, and a final extension of 10 min at 72°C	Guerber et al., 2003
		GDR1	Reverse	GGGTGGAGTCGTACTTGAGCATGT		Guerber et al., 2003
ACT	Actin	ACT-512F	Forward	ATGTGCAAGGCCGGTTTCGC	Denaturation for 4 min at 94°C, followed by 30 cycles; 30 s at 94°C, 30 s at 57°C, 30 s at 72°C, and a final extension of 10 min at 72°C	Carbone and Kohn, 1999
		ACT-783R	Reverse	TACGAGTCCTTCTGGCCCAT		Carbone and Kohn, 1999
TUB	β-tubulin	T1	Forward	AACATGCGTGAGATTGTAAGT	Denaturation for 4 min at 94°C, followed by 30 cycles; 30 s at 94°C, 30 s at 61°C, 30 s at 72°C, and a final extension of 10 min at 72°C	O'Donnell and Cigelnik, 1997
		Bt-2b	Reverse	ACCCTCAGTGTAGTGACCCTTGGC		Glass and Donaldson, 1995
CAL	Calmodulin	CL1A	Forward	GATCAAGGAGGCCTTCTC	Denaturation for 4 min at 94°C, followed by 30 cycles; 30 s at 94°C, 30 s at 58°C, 30 s at 72°C, and a final extension of 10 min at 72°C	O'Donnell et al., 2000
		CL2A	Reverse	TTTTTGCATCATGAGTTGGAC		O'Donnell et al., 2000
CHS-1	Chitin synthase 1	CHS-79F	Forward	TGGGGCAAGGATGCTTGGAAGAAG	Denaturation for 4 min at 94°C, followed by 30 cycles; 30 s at 94°C, 30 s at 58°C, 30 s at 72°C, and a final extension of 10 min at 72°C	Carbone and Kohn, 1999
		CHS-354R	Reverse	TGGAAGAACCATCTGTGAGAGTTG		Carbone and Kohn, 1999
GS	Glutamine synthetase	GSLF2	Forward	TACACGAGSAAAAGGATACGC	Denaturation for 4 min at 94°C, followed by 30 cycles; 30 s at 94°C, 30 s at 54°C, 30 s at 72°C, and a final extension of 10 min at 72°C	Liu et al., 2016
		GSLR1	Reverse	AGRCGCACATTGTCAGTATCG		Liu et al., 2016
ApMat	Apn2-Mat1-2	AM-F	Forward	TCATTCTACGTATGTGCCCG	Denaturation for 3 min at 94°C, followed by 30 cycles; 45 s at 94°C, 45 s at 62°C, 1 min at 72°C, and a final extension of 7 min at 72°C	Silva et al., 2012
		AM-R	Reverse	CCAGAAATACACCGAACTTGC		Silva et al., 2012

Disease incidence was determined at 10 dpi, while the incubated leaves were monitored for the onset of anthracnose lesions for up to 20 dpi. Virulence was determined by measuring the diameter of the necrotic lesions in two perpendicular directions at 7 and 10 dpi for the wounded and non-wounded leaves, respectively. Differences in the virulence of the isolates were determined by ANOVA, and mean values were compared by Tukey's test ($P < 0.05$) using SPSS as previously described. Each *Colletotrichum* isolate involved in the virulence test was reisolated from the inoculated leaves, and their identity was confirmed by morphological and molecular approaches as previously described to fulfill Koch's postulates.

Biofungicide Sensitivity Assessments *in vitro*

Effects on Mycelial Growth

Phenazine-1-carboxylic acid [1% active ingredient (a.i.); Shanghai Non-gle Biological Products Co., Ltd., Shanghai, China], tetramycin (0.3% a.i.; Liaoning Wkioc Bioengineering Co., Ltd., Liaoning, China), and kasugamycin (4% a.i.; Shaanxi Microbe Biotechnology Co., Ltd., Shaanxi, China) were used. Fourteen representative isolates were selected based on the above studies. The fungicide sensitivity of each isolate was tested on complete medium (CM) plates (Yeast extract 10 g/L, Casamino-acid 5 g/L, Agar 15 g/L, 1% sterile glucose after autoclaving) amended with fungicides. Mycelial blocks (2 mm in side length) aseptically taken from actively growing cultures were placed onto CM with or without (control) fungicide amendments. The final concentrations of each a.i. in the amended media were 0.1, 0.25, 0.5, 1, 2.5, and 5 μg/mL for tetramycin and 1, 2.5, 5, 10, 25, and 50 μg/mL for PCA and kasugamycin. Each treatment was tested in triplicate, and the entire experiment was repeated twice. The mean colony diameter was measured at 4 dpi, and the formula for percent inhibition was [(radial growth of the control – radial growth at fungicide concentration)/radial growth of the control] × 100%. Half of the maximal effective

TABLE 3 | Morphological characteristics of *Colletotrichum* isolates from *Cyclocarya paliurus*.

Species/Isolate	Conidia		Appressoria		Ascospore		
	Length (μm)	Width (μm)	Length (μm)	Width (μm)	Length (μm)	Width (μm)	Shape
C. aenigma							
HC3	18.58 ± 0.51ab (14.79–26.09)	7.44 ± 0.17b (5.56–10.2)	10.71 ± 0.25ab (8.35–13.68)	7.48 ± 0.18f (5.85–9.56)	18.4 ± 0.3bc (16.04–22.36)	7.32 ± 0.14a (6.11–9.06)	Cylindrical
SC7	18.82 ± 0.45ab (15.74–26.64)	8.17 ± 0.23a (5.73–11.13)	11.46 ± 0.42a (8.61–16.92)	7.96 ± 0.25abcde (5.87–11.73)	18.7 ± 0.24abc (16.91–21.94)	7.44 ± 0.14a (6.01–8.85)	Cylindrical
YM8	19.29 ± 0.43a (14.3–24.64)	8.29 ± 0.17a (6.44–10.97)	11.2 ± 0.24ab (9.6–14.34)	7.53 ± 0.14ab (5.87–9.06)	17.77 ± 0.16c (15.94–19.52)	6.75 ± 0.15b (5.56–9.17)	Cylindrical
C. fructicola							
BM5	16.24 ± 0.24d (12–18.68)	6.52 ± 0.17d (4.79–8.28)	10.7 ± 0.21ab (8.35–13.84)	7.79 ± 0.12bcdef (6.45–9.4)	19.55 ± 0.33a (16.67–23.75)	4.63 ± 0.08c (3.85–5.44)	Curved fusoid
GX1	16.52 ± 0.38d (13.64–23.14)	6.9 ± 0.19bcd (5.1–9.79)	10.75 ± 0.25ab (8.67–14.15)	7.88 ± 0.13bcdef (6.53–9.56)	19.3 ± 0.38ab (15.41–25.35)	4.68 ± 0.11c (3.59–5.81)	Curved fusoid
HC2	17.11 ± 0.42cd (12.39–22.34)	7.35 ± 0.16b (5.63–9.59)	10.87 ± 0.23ab (9.02–13.49)	7.83 ± 0.13bcdef (6.56–9.25)	18.82 ± 0.36ab (13.23–21.34)	4.72 ± 0.12c (3.4–5.84)	Curved fusoid
LC7	17.07 ± 0.24cd (14.44–19.92)	7.03 ± 0.17bcd (5.47–8.77)	10.97 ± 0.2ab (9.24–12.94)	7.69 ± 0.14def (6.55–8.97)	19.2 ± 0.34ab (14.32–24.04)	4.67 ± 0.11c (3.79–6.13)	Curved fusoid
NC25	16.38 ± 0.4d (12.89–22.79)	6.72 ± 0.18d (4.89–8.66)	11.17 ± 0.19ab (9.33–12.91)	7.77 ± 0.14cdef (6.54–9.26)	19.05 ± 0.37ab (16.53–23.89)	4.55 ± 0.09c (3.2–5.65)	Curved fusoid
SC6	16.68 ± 0.29cd (13.49–20.71)	6.58 ± 0.16d (4.5–8.25)	10.42 ± 0.23b (8.49–12.86)	7.86 ± 0.11bcdef (6.61–8.95)	19.06 ± 0.39ab (13.64–24.69)	4.68 ± 0.12c (3.1–6.19)	Curved fusoid
YH6	16.61 ± 0.38cd (14.36–22.58)	6.68 ± 0.17d (4.95–8.83)	10.68 ± 0.25ab (8.04–12.95)	7.99 ± 0.14abcde (6.76–9.97)	18.8 ± 0.31ab (15.41–21.99)	4.72 ± 0.12c (3.7–6.13)	Curved fusoid
C. gloeosporioides							
BM6	17.07 ± 0.28cd (14.72–19.84)	6.76 ± 0.16cd (5.15–8.45)	11.05 ± 0.2ab (9.55–13.48)	8.27 ± 0.15ab (6.94–10.39)	13.24 ± 0.3d (10.66–16.8)	4.83 ± 0.09c (3.91–5.98)	Cylindrical
GX3	17.25 ± 0.37cd (13.44–23.81)	6.93 ± 0.12bcd (5.87–8.1)	11.12 ± 0.18ab (9.13–13.01)	8.1 ± 0.16abcd (6.06–10.61)	13.14 ± 0.32d (9.86–17.07)	4.81 ± 0.09c (3.62–5.84)	Cylindrical
LC2	16.96 ± 0.26cd (15.06–21.22)	7.04 ± 0.16bcd (4.95–9.69)	11.18 ± 0.18ab (9.48–13.12)	8.24 ± 0.14abc (6.94–10.11)	12.9 ± 0.33d (9.02–16.54)	4.89 ± 0.09c (3.79–5.84)	Cylindrical
YM4	17.76 ± 0.33bc (15.69–24.82)	7.26 ± 0.13bc (5.96–8.67)	11.1 ± 0.21ab (9.63–13.91)	8.38 ± 0.12a (6.99–10.16)	13.23 ± 0.29d (10.73–16.06)	4.85 ± 0.08c (4.19–5.98)	Cylindrical

Data are mean ± standard error, with ranges in parentheses.
Columns with the same letter do not differ significantly according to Duncan's test ($P < 0.05$).

concentration (EC_{50}) was estimated by regression to the $\log_{10}$ probability conversion of the percentage of inhibition of the fungicide concentrations.

Effects on Spore Germination

Tetramycin was selected to test its ability to inhibit conidia germination. Spore suspensions and fungicide solutions were mixed with sterilized water to 10 mL volume. The final fungicide concentrations were 0.005, 0.01, 0.05, 0.1, 0.5, and 1 μg/mL, while spore suspension was adjusted to 1×10^5 spores/mL for each treatment. A 20 μL droplet of each suspension was placed on a hydrophobic cover slip and incubated at 25°C for 18–20 h in a humidity chamber according to Fang et al. (2018). Each treatment was conducted in triplicate, and the entire experiment was repeated twice. Conidia were then observed at ×100 magnification using a ZEISS microscope and scored as germinated if the length of the germ tube was longer than half of the conidial length. The conidial germination inhibition rate was calculated as previously described (Munir et al., 2016).

RESULTS

Field Symptoms and *Colletotrichum* Isolates

In May 2018, typical symptoms of anthracnose were first observed on newly emerged leaves of *C. paliurus* in a commercial nursery in Baima (**Figure 1A**), and the infection quickly spread to all *C. paliurus* nurseries within the growing season, with the infection rate reaching 64% (150 trees were investigated). Similar symptoms were observed in plant bases at Changzhou and Yancheng, with infection rates over 35 and 45% (100 trees were investigated), respectively. The initial symptoms appeared in the form of subcircular or irregular pale-brown spots scattered on the leaves (**Figure 1C**). Gradually, the lesions enlarged and coalesced to form large necrotic areas, which turned off-white surrounded by a dark-brown border as symptoms progressed (**Figure 1B**). The dead tissue withered, resulting in premature defoliation of the plant in severe cases (**Figure 1A**). Under high-moisture conditions, a number of acervuli were formed in concentric rings and oozed gelatinous orange spore

masses (**Figure 1D**). Photomicrographs further corroborated the presence of conidiophores and conidia on the surfaces of leaf lesions under optical or SEM microscopy (**Figures 1E,F**).

A total of 44 monosporic *Colletotrichum* isolates were recovered from symptomatic tissues and used for further molecular identification (**Table 1**). The shapes and sizes of conidia of these cultures were basically concordant with the sporulation on the lesions (**Figures 2C**, **3C**, **4C**). The general morphological characteristics of all isolates resembled those of *Colletotrichum* species.

Molecular Identification and Phylogenetic Analysis

In the present study, the ITS, CAL, ACT, GPDH, TUB, CHS-1, GS, and ApMat region/genes of all 44 monosporic isolates were successfully amplified and sequenced (**Table 1**). Sequences generated herein along with reference sequences from ex-type or other authoritative specimens were concatenated for phylogeny construction, composing a dataset of 3192 characters, with 1828 constant characters, 574 parsimony-uninformative characters, and 790 parsimony-informative characters.

The topological structure of the phylogenetic trees constructed using BI and ML criteria was basically consistent, demonstrating that the evolutionary relationships of the experimental strains were statistically supported. A consensus tree with clade support from bootstrap proportions (BPs) and PP values was generated (**Figure 5**). The phylogenetic tree revealed that all 44 *Colletotrichum* isolates belonged to three well-separated clades and nested within the *C. gloeosporioides* species complex. Six *Colletotrichum* isolates composed a highly supported clade (100% BP/1.00 PP) with the *Colletotrichum aenigma* type strain ICMP 18608. Twenty-eight isolates belonged to the other highly supported clade (100% BP/1.00 PP) along with the *Colletotrichum fructicola* type strain ICMP 18581. Ten isolates clustered in another highly supported clade (100% BP/1.00 PP) with the *C. gloeosporioides* s. s. type strain IMI 356878 (**Figure 5**).

Morphological and Biological Analyses

Fourteen representative isolates clustered in three clades in the ML/BI phylogenetic analysis, including three of *C. aenigma*, seven of *C. fructicola*, and four of *C. gloeosporioides* s. s., were selected for further studies (**Table 1**).

Colonies of *C. fructicola* isolates produced abundant grayish-green aerial hyphae with white halo edges, and the back of the colony was grayish-green with concentric rings (**Figures 3A,B**). Isolates of *C. aenigma* and *C. gloeosporioides* s. s. exhibited white or gray mycelia, and the back of the colony was densely arranged with a grayish-green color in the center (**Figures 2A,B**, **4A,B**). There were few differences in the shapes of conidia, conidiophores, and appressoria among the three species. Conidia were all one-celled, hyaline, smooth-walled, mostly cylindrical with broadly rounded ends, and sometimes slightly and gradually acute to the end (**Figures 2C**, **3C**, **4C**). The average conidial sizes for isolates were as follows: *C. aenigma*, 14.3–26.6 × 5.56–11.13 μm; *C. fructicola*, 12–23.14 × 4.5–9.79 μm; and *C. gloeosporioides* s. s., 13.44–24.82 × 4.95–9.69 μm (**Table 3**). Conidiophores were smooth-walled, septate, and hyaline to pale brown

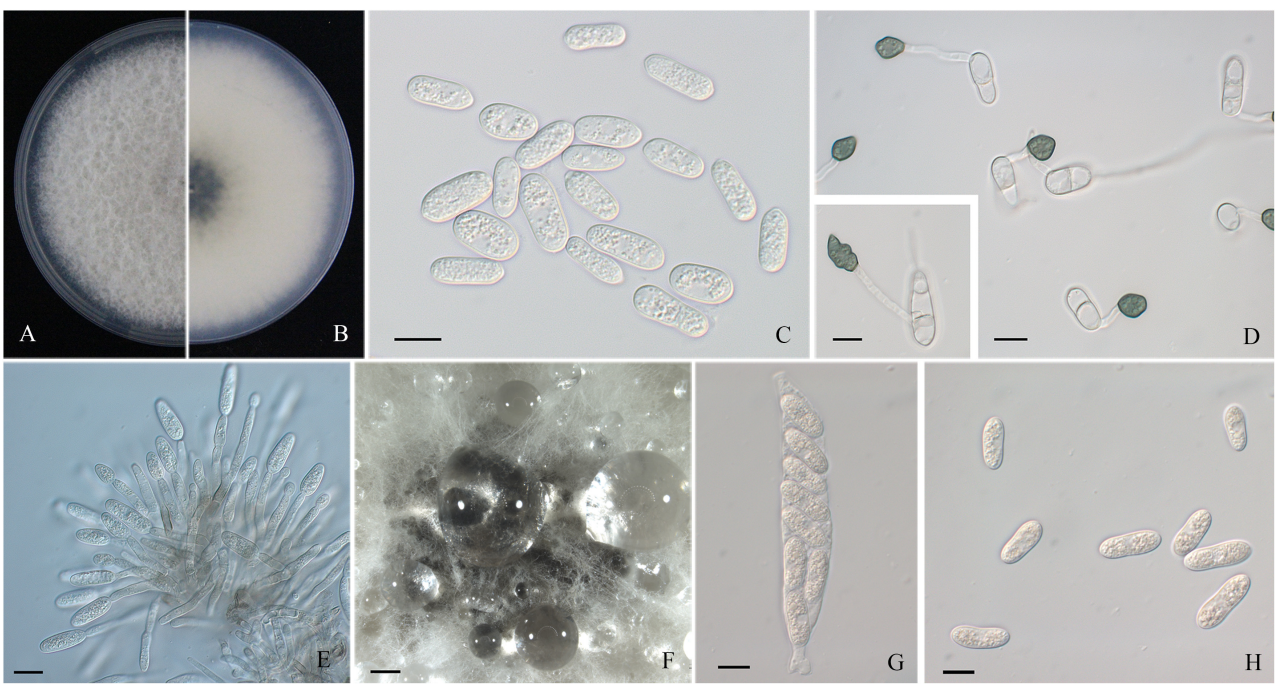

FIGURE 2 | Morphological characters of *Colletotrichum aenigma*. **(A,B)** Front and back view, respectively, of 6-days-old PDA culture. **(C)** Conidia. **(D)** Appressoria. **(E)** Conidiophores. **(F)** Ascomata developed on PDA plates. **(G)** Asci. **(H)** Ascospores. Scale bars: **(C–E,G,H)** = 10 μm; **(F)** = 500 μm.

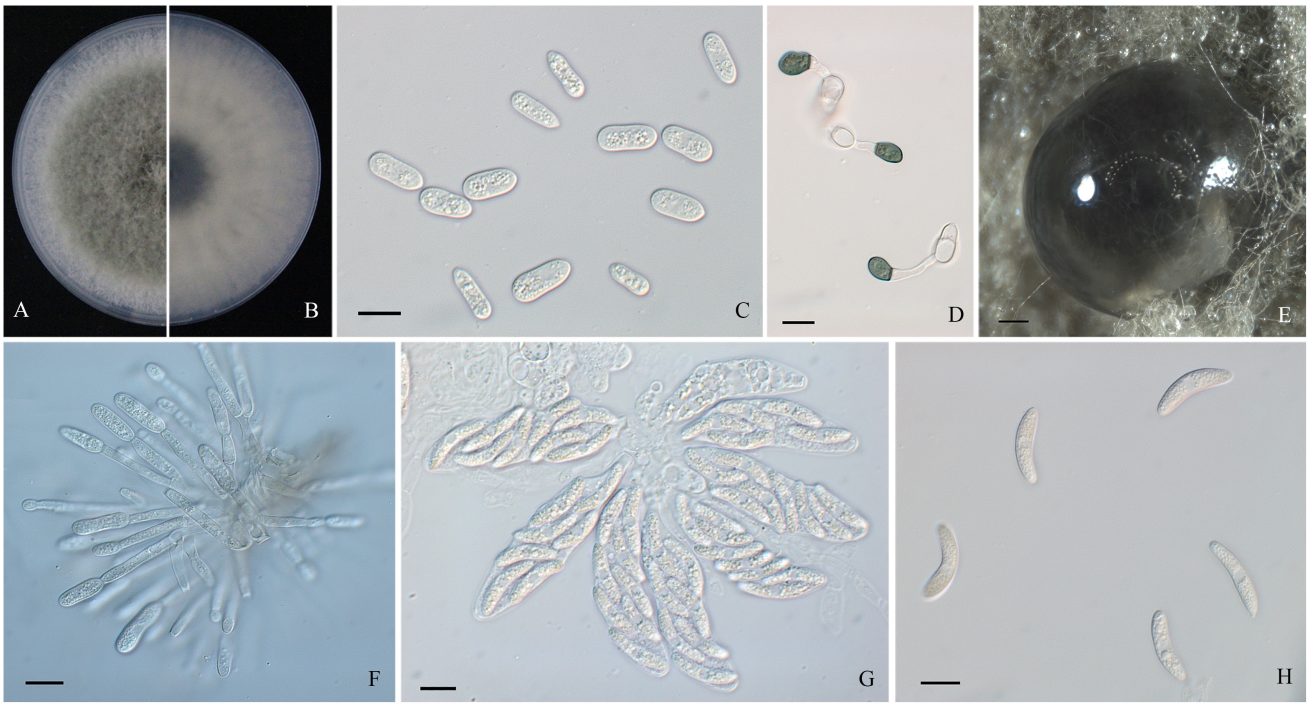

FIGURE 3 | Morphological characters of *Colletotrichum fructicola*. **(A,B)** Front and back view, respectively, of 6-days-old PDA culture. **(C)** Conidia. **(D)** Appressoria. **(E)** Ascomata developed on PDA plates. **(F)** Conidiophores. **(G)** Asci. **(H)** Ascospores. Scale bars: **(C,D,F–H)** = 10 μm; **(E)** = 200 μm.

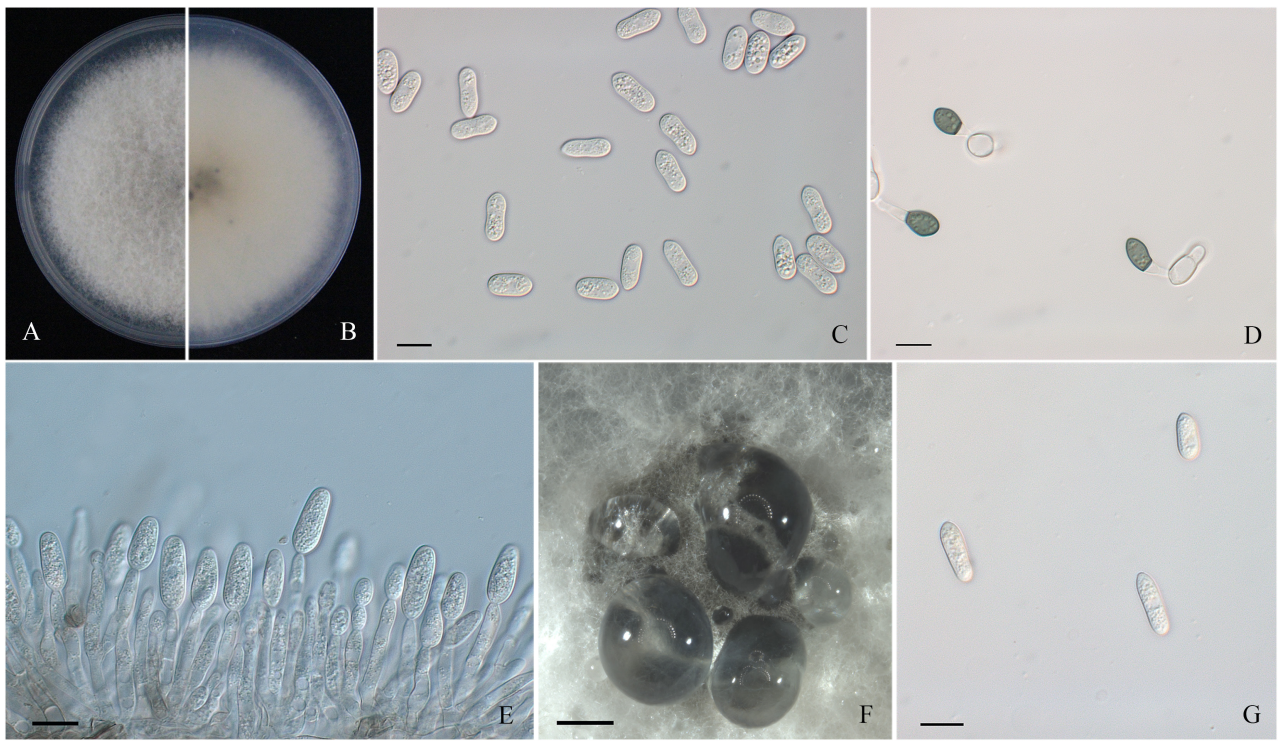

FIGURE 4 | Morphological characters of *Colletotrichum gloeosporioides* sensu stricto. **(A,B)** Front and back view, respectively, of 6-days-old PDA culture. **(C)** Conidia. **(D)** Appressoria. **(E)** Conidiophores. **(F)** Ascomata developed on PDA plates. **(G)** Ascospores. Scale bars: **(C–E,G)** = 10 μm; **(F)** = 500 μm.

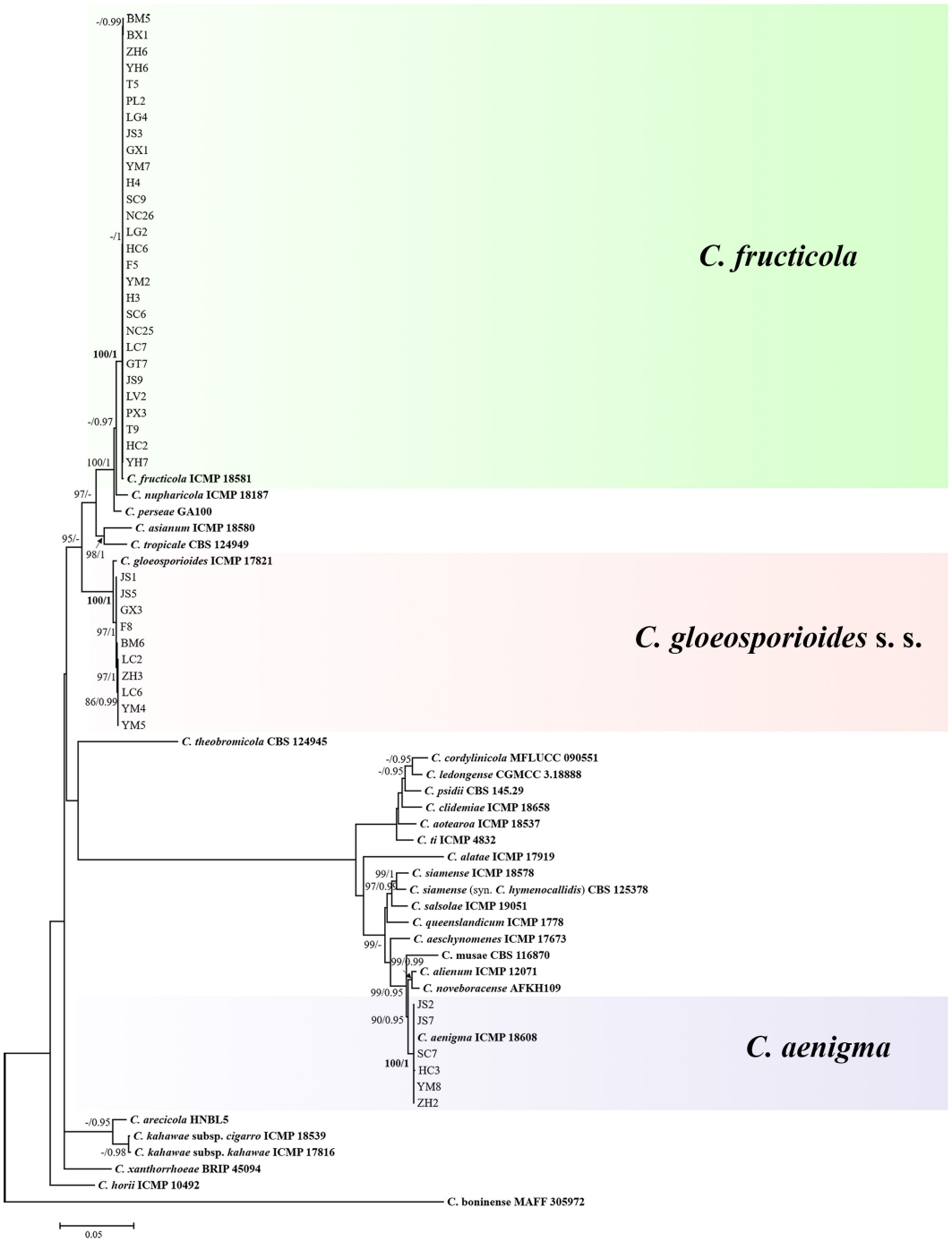

FIGURE 5 | Maximum-likelihood phylogenetic tree of 66 isolates of the *Colletotrichum gloeosporioides* species complex. The tree was built using concatenated sequences of the ITS, GAPDH, CAL, ACT, CHS-1, TUB, GS, and ApMat region or genes, each with a separate model of DNA evolution. The tree generated by Bayesian inference had a similar topology. Bootstrap support values above 85% and Bayesian posterior probability values above 0.95 are shown at the nodes. Ex-type or other authoritative cultures are emphasized in bold font. *C. boninense* (MAFF 305972) was used as an outgroup. The scale bar indicates the average number of substitutions per site.

(**Figures 2E**, **3F**, **4E**). Appressoria were dark brown, subglobose or ellipsoid, and rarely irregular (**Figures 2D**, **3D**, **4D**). The average appressorium sizes for the isolates were as follows: *C. aenigma*, 8.35–16.92 × 5.87–11.73 μm; *C. fructicola*, 8.04–14.15 × 6.45–9.97 μm; and *C. gloeosporioides* s. s., 9.13–13.91 × 6.06–10.61 μm (**Table 3**). Ascomata of three *Colletotrichum* species formed on PDA at 20 dpi and were semi-immersed in agar medium, dark-brown, and subglobose

to pyriform (**Figures 2F**, **3E**, **4F**). Asci were clavate, fasciculate, and eight-spored in most cases, while asci of *C. gloeosporioides* s. s. were not observed (**Figures 2G**, **3G**). Ascospores of *C. aenigma* isolates were hyaline, smooth-walled, aseptate, cylindrical, and 15.94–22.36 × 5.56–9.17 μm in size (**Table 3** and **Figure 2H**). Ascospores of *C. gloeosporioides* s. s. isolates were hyaline, smooth-walled, aseptate, cylindrical, and 9.02–17.07 × 3.62–5.98 μm in size (**Table 3** and **Figure 4G**). Ascospores of *C. fructicola* were hyaline, aseptate, smooth-walled, fusoid, slightly curved, straight with round ends, and 13.23–25.35 × 3.1–6.19 μm in size (**Table 3** and **Figure 3H**).

All 14 representative isolates tested exhibited a similar growth pattern on PDA at the different treatment temperatures. No mycelial growth of any tested isolates was observed *in vitro* at 5°C. The optimum mycelial growth temperature of the three *Colletotrichum* species was 25–30°C, but the high temperature tolerance of the three species was different. Isolates of *C. aenigma* and *C. fructicola* were more sensitive to high temperature and grew very slowly (or could not grow) at 40°C, with mean growth rates lower than those of *C. gloeosporioides* s. s. isolates.

Virulence Tests of *Colletotrichum* Isolates

All 14 selected isolates were pathogenic on leaves of *C. paliurus* and reproduced typical symptoms of anthracnose. Seven days after wounded or non-wounded inoculation, distinct brown or off-white necrotic lesions with dark-brown boundaries developed (**Figure 6**), while no symptoms developed on the corresponding mock controls.

The severity of disease caused by these isolates showed significant differences (**Table 4**). Isolates of *C. gloeosporioides* s. s. generally showed strong virulence, with mean lesion diameters ranging from 17.88 to 23.16 and 17.52 to 22.11 mm with wounded and non-wounded inoculation using mycelial plugs as inocula, respectively. There was no significant difference in virulence among *C. fructicola* isolates in *C. paliurus* leaves, with mean lesion diameters ranging from 16.65 to 20.52 and 17.41 to 21.09 mm with wounded and non-wounded inoculation using mycelial plugs as inocula, respectively. *C. aenigma* isolates showed much weaker virulence, with mean lesion diameters ranging from 12.38 to 14.89 and 11.78 to 14.12 mm with wounded and non-wounded inoculation using mycelial plugs as inocula, respectively. The lesions produced by mycelial inoculation were generally larger than those produced by spore suspension inoculation among the three *Colletotrichum* species (**Table 4**). *Colletotrichum gloeosporioides* s. s. isolate BM6 and *C. fructicola* isolate BM5 produced reproductive structures of the fungus on the necrotic lesions (**Figure 6**). *C. fructicola* isolate YH6 produced lesions with a wheel-shaped pattern on *C. paliurus* leaves (**Figure 6**). The *Colletotrichum* species were reisolated from all inoculated symptomatic leaves and were found to be morphologically and molecularly identical to the original isolates using the aforementioned methods, thus fulfilling Koch's postulates.

Sensitivity of *Colletotrichum* Isolates to Biofungicides

Fourteen representative isolates evaluated showed similar biological responses to all tested biofungicides. Kasugamycin at 50 mg/mL showed no suppressive activity against the mycelial growth of the three *Colletotrichum* spp. on CM medium (EC_{50} > 100 μg/mL). PCA showed moderate inhibition of the

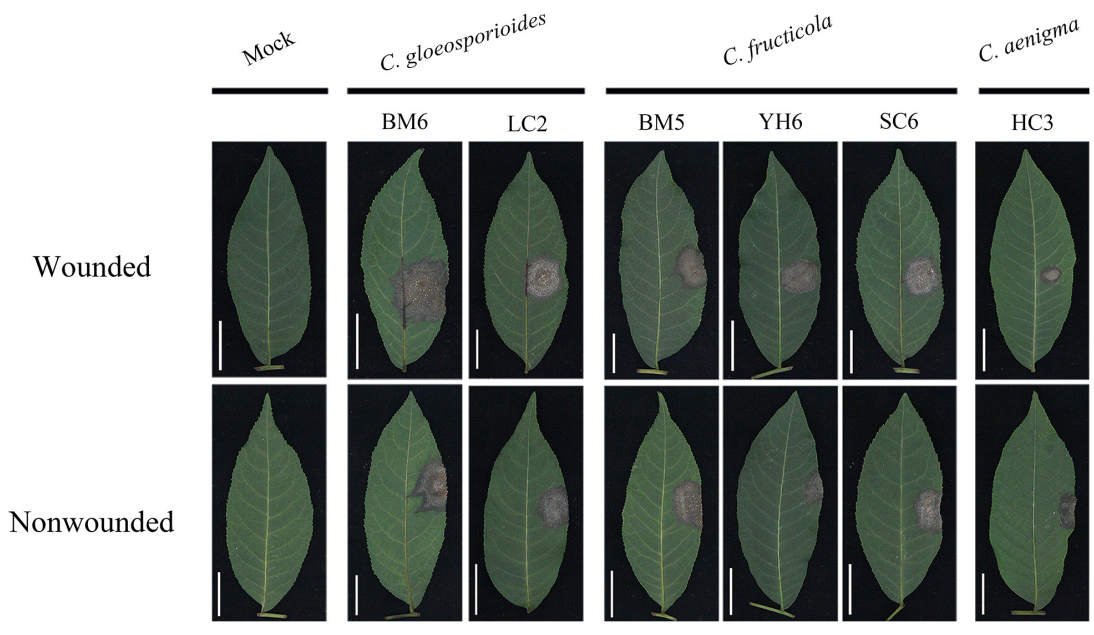

FIGURE 6 | Typical symptoms induced by mycelial discs of representative isolates of *C. gloeosporioides* sensu stricto, *C. fructicola*, and *C. aenigma* on wounded (upper) and unwounded (lower) detached leaves of *Cyclocarya paliurus*.

TABLE 4 | Pathogenicity of *Colletotrichum* isolates on detached leaves of *Cyclocarya paliurus*.

Species/ Isolates	Infected leaves (%)[a]				Lesion diameter (mm)[b]			
	Conidial suspension		Mycelial plug		Conidial suspension		Mycelial plug	
	Wounded	Non-wounded	Wounded	Non-wounded	Wounded	Non-wounded	Wounded	Non-wounded
CK	–	–	–	–	–	–	–	–
C. aenigma								
HC3	80.00 ± 11.55	60.00 ± 0.00	100.00 ± 0.00	86.67 ± 6.67	9.63 ± 0.9*b*	5.79 ± 0.56*b*	12.38 ± 1.10*f*	14.12 ± 1.28*cd*
SC7	93.33 ± 6.67	60.00 ± 0.00	100.00 ± 0.00	93.33 ± 6.67	9.58 ± 0.96*b*	5.77 ± 0.48*b*	13.10 ± 0.82*ef*	14.44 ± 0.92*cd*
YM8	73.33 ± 6.67	66.67 ± 6.67	100.00 ± 0.00	86.67 ± 6.67	8.9 ± 0.81*b*	5.41 ± 0.39*b*	14.89 ± 1.07*def*	11.78 ± 1.02*d*
C. fructicola								
BM5	93.33 ± 6.67	80.00 ± 11.55	100.00 ± 0.00	100.00 ± 0.00	17.69 ± 0.99*a*	15.85 ± 1.26*a*	20.52 ± 0.61*abc*	20.37 ± 0.91*ab*
GX1	93.33 ± 6.67	73.33 ± 6.67	100.00 ± 0.00	93.33 ± 6.67	16.44 ± 1.07*a*	13.85 ± 1.26*a*	18.75 ± 0.76*bcd*	20.16 ± 0.98*ab*
HC2	86.67 ± 6.67	80.00 ± 11.55	100.00 ± 0.00	100.00 ± 0.00	16.41 ± 1.16*a*	13.86 ± 1.27*a*	18.18 ± 1.06*bcd*	19.75 ± 1.03*abc*
LC7	86.67 ± 6.67	86.67 ± 6.67	100.00 ± 0.00	93.33 ± 6.67	16.21 ± 1.03*a*	14.73 ± 1.49*a*	20.51 ± 0.94*abc*	18.59 ± 1.76*abc*
NC25	93.33 ± 6.67	86.67 ± 13.33	100.00 ± 0.00	93.33 ± 6.67	16.34 ± 0.88*a*	13.41 ± 1.03*a*	18.93 ± 1.07*bcd*	21.09 ± 0.95*a*
SC6	93.33 ± 6.67	73.33 ± 6.67	100.00 ± 0.00	93.33 ± 6.67	15.45 ± 1.16*a*	12.93 ± 1.52*a*	16.90 ± 0.94*cde*	18.06 ± 1.54*abc*
YH6	93.33 ± 6.67	80.00 ± 11.55	100.00 ± 0.00	100.00 ± 0.00	15.56 ± 1.04*a*	13.87 ± 1.12*a*	16.65 ± 0.87*cde*	17.41 ± 1.14*abc*
C. gloeosporioides								
BM6	86.67 ± 6.67	80.00 ± 11.55	100.00 ± 0.00	100.00 ± 0.00	18.43 ± 0.93*a*	15.92 ± 1.14*a*	23.16 ± 0.80*a*	22.11 ± 0.66*a*
GX3	86.67 ± 6.67	86.67 ± 6.67	100.00 ± 0.00	100.00 ± 0.00	17.24 ± 0.91*a*	16.35 ± 0.87*a*	20.29 ± 0.81*abc*	19.03 ± 1.03*abc*
LC2	86.67 ± 6.67	80.00 ± 11.55	100.00 ± 0.00	100.00 ± 0.00	17.27 ± 0.97*a*	12.98 ± 0.86*a*	17.88 ± 0.61*bcd*	17.52 ± 1.68*abc*
YM4	93.33 ± 6.67	80.00 ± 11.55	100.00 ± 0.00	100.00 ± 0.00	17.44 ± 0.63*a*	15.21 ± 1.49*a*	20.40 ± 0.58*abc*	21.39 ± 1.03*a*

[a,b]*Values were means ± standard error of three replications.*
Means with different letters indicate mean lesion lengths that are significantly different ($P < 0.05$). Data were calculated using disease incidence of 15 inoculated leaves.
– represents no symptom developed on inoculated site.
[CK]*Detached C. paliurus leaves were inoculated with sterile water or PDA plugs without the pathogens (as controls).*

mycelial growth of the three *Colletotrichum* spp., with isolates of *C. fructicola* exhibiting more sensitivity to this biofungicide. The EC_{50} of tetramycin against the mycelial growth of all representative isolates was lower than that of any of the other biofungicides, including the low EC_{50} of tetramycin against spore germination, indicating that tetramycin was the most effective biofungicide against the three *Colletotrichum* spp. used in this study.

DISCUSSION

In recent years, the cultivation of *C. paliurus* has undergone a major expansion to meet the increasing demand for young leaves of this species for medical use or *C. paliurus* tea production in China, which may have caused the high incidence of foliar diseases in these newly established plantations. Therefore, it is of great importance to diagnose and control these fungal diseases of *C. paliurus*. Unfortunately, little information was available about these diseases, i.e., *C. paliurus* anthracnose. Hitherto, this study is first comprehensive analysis demonstrating the etiology of *C. paliurus* anthracnose in China, providing valuable information about the phenotypic and molecular characteristics, virulence, and fungicide sensitivity of the causal agents associated with this disease. Moreover, this study provides the first report of *C. aenigma*, *C. fructicola*, and *C. gloeosporioides* s. s. causing *C. paliurus* anthracnose in China as well as in the world.

Colletotrichum gloeosporioides species complex is regarded as the most challenging taxa within the *Colletotrichum* genus (Silva et al., 2012). Although polyphasic method is recommended for characterizing *Colletotrichum* species, there is still lack of consensus among taxonomists on the selection of markers for phylogenetic studies (Cao et al., 2020; Vieira et al., 2020). Recent studies revealed that concatenated GS and ApMat alignment can achieve a satisfactory *Colletotrichum* species identification (Liu et al., 2015; Sharma et al., 2017). Conservative region/genes (ITS, GAPDH, CAL, CHS-1, ACT, and TUB) have been previously accepted for delimiting species in this species complex (Weir et al., 2012). Therefore, in the present study, eight loci (ITS, GAPDH, CAL, CHS-1, ACT, TUB, including GS and ApMat) were selected in phylogenetic analysis for *Colletotrichum* isolates classification. Based on BI/ML multilocus concatenated phylogenetic analyses, including sequences from 28 authentic specimens in the *C. gloeosporioides* species complex, the 44 isolates were categorized into three well-separated clades: six isolates clustered in the *C. aenigma* clade (14%), 28 isolates clustered in the *C. fructicola* clade (64%), and 10 isolates clustered in the *C. gloeosporioides* s. s. clade (22%). With respect to phenotypic characterization based on colony morphology, characteristics of conidia, appressoria, ascospores, and asci were entirely in line with the results of the molecular data.

Colletotrichum fructicola was first described by Prihastuti et al. (2009), causing coffee berry disease in Thailand. The species is geographically diverse and threatens a wide range of hosts, which has been reported on *Fragaria* × *ananassa*

TABLE 5 | Growth rate (mm/4d) of *Colletotrichum* isolates from *Cyclocarya paliurus* cultured on PDA at different temperatures.

Species/Isolates	5°C	10°C	15°C	20°C	25°C	30°C	35°C	40°C
C. aenigma								
HC3	0a	2.01 ± 0.1*ab*	3.92 ± 0.09*abc*	7.67 ± 0.01*abc*	12.43 ± 0.14*b*	12.39 ± 0.14*a*	7.6 ± 0.57*a*	2.4 ± 1.22*ab*
SC7	0a	2.26 ± 0.2*a*	3.77 ± 0.12*abc*	7.66 ± 0.04*abc*	12.66 ± 0.19*b*	12.62 ± 0.09*a*	7.69 ± 0.08*a*	2.13 ± 1.11*ab*
YM8	0a	2.24 ± 0.17*a*	3.79 ± 0.15*abc*	7.96 ± 0.05*abc*	12.28 ± 0.31*b*	12.19 ± 0.08*a*	7.72 ± 0.56*a*	0*b*
C. fructicola								
BM5	0a	1.11 ± 0.56*ab*	3.54 ± 0.22*abc*	8.81 ± 0.09*ab*	15.49 ± 0.04*a*	12.93 ± 0.28*a*	5.64 ± 0.48*b*	2.71 ± 1.36*ab*
GX1	0a	1.79 ± 0.12*ab*	3.61 ± 0.09*abc*	8.32 ± 0.28*abc*	15.81 ± 0.04*a*	13.56 ± 0.25*a*	5.17 ± 0.42*b*	2.71 ± 1.35*ab*
HC2	0a	1.62 ± 0.18*ab*	3.2 ± 0.19*abc*	8.46 ± 0.49*abc*	15.42 ± 0.12*a*	13.33 ± 0.27*a*	4.91 ± 0.08*b*	0*b*
LC7	0a	1.36 ± 0.14*ab*	3.72 ± 0.16*abc*	8.96 ± 0.07*a*	15.84 ± 0.07*a*	12.99 ± 0.45*a*	5.59 ± 0.11*b*	1.99 ± 0.05*ab*
NC25	0a	0.91 ± 0.46*b*	3.35 ± 0.19*abc*	8.56 ± 0.35*abc*	15.68 ± 0.13*a*	12.93 ± 0.34*a*	5.36 ± 0.46*b*	2.66 ± 1.33*ab*
SC6	0a	1.68 ± 0.28*ab*	3.27 ± 0.35*bc*	8.12 ± 0.17*abc*	15.74 ± 0.17*a*	13.45 ± 0.45*a*	5.44 ± 0.34*b*	0*b*
YH6	0a	1.61 ± 0.21*ab*	3.64 ± 0.24*abc*	8.28 ± 0.35*abc*	15.9 ± 0.15*a*	13.42 ± 0.14*a*	5.7 ± 0.47*b*	2.08 ± 0.13*ab*
C. gloeosporioides								
BM6	0a	1.84 ± 0.07*ab*	4.27 ± 0.13*a*	7.37 ± 0.38*c*	11.54 ± 0.36*bc*	12.37 ± 0.65*a*	8.12 ± 0.21*a*	3.36 ± 0.99*ab*
GX3	0a	1.89 ± 0.17*ab*	4.21 ± 0.2*ab*	7.62 ± 0.13*bc*	11.62 ± 0.46*bc*	12.66 ± 0.17*a*	8.35 ± 0.2*a*	5.25 ± 1.13*a*
LC2	0a	1.76 ± 0.19*ab*	4.24 ± 0.13*a*	7.57 ± 0.29*bc*	10.88 ± 0.26*c*	11.75 ± 0.18*a*	8.1 ± 0.12*a*	3.2 ± 0.76*ab*
YM4	0a	1.93 ± 0.19*ab*	4.26 ± 0.17*a*	7.73 ± 0.38*abc*	12.04 ± 0.43*bc*	12.42 ± 0.8*a*	8.01 ± 0.15*a*	2.43 ± 0.74*ab*

Columns with the same letter do not differ significantly according to Tukey's test ($P < 0.05$).

and *Malus* sp. (United States), *Ficus* sp. (Germany), *Persea americana* (Australia), *Pyrus pyrifolia* (Japan), *Limonium* sp. (Israel), *Tetragastris* sp. and *Theobroma* sp. (Panama), *Dioscorea* sp. (Nigeria), *Malus* sp. (Brazil) (Weir et al., 2012), and *Mangifera indica* (China) (Mo et al., 2018). In the current study, *C. fructicola* was the most predominant species and exhibited strong pathogenicity (**Table 4**), which seems to be the most economically harmful species of *C. paliurus* anthracnose in Jiangsu Province, China.

Colletotrichum gloeosporioides s. s., a genetically and biologically diverse species, previously reported to infect fruits in tropical area (Sangeetha and Rawal, 2008; Udayanga et al., 2013), which is probably related to its ability to tolerate high temperatures (**Table 5**). However, this species was recently reported increasingly prevalent in the temperate region, such as Hebei, Shandong, and Shanxi Provinces of China (Jayawardena et al., 2016; Wang et al., 2020). Results in the present study demonstrated that *C. gloeosporioides* showed the strongest pathogenicity to *C. paliurus* (**Table 4**). The prevalence and ecological adaptation zone of *C. gloeosporioides* on *C. paliurus* in China would be further studied.

Interestingly, multiple *Colletotrichum* species were isolated and identified from the same leaf and even within the same lesion of single *C. paliurus* trees. As reported in previous studies, several *Colletotrichum* species can cause anthracnose on the same host (Munir et al., 2016; Chen Y. et al., 2017; De Silva et al., 2017a; Diao et al., 2017; Guarnaccia et al., 2017; Fu et al., 2019; Xue et al., 2019). It is reasonable to believe that *C. paliurus* anthracnose may be a complex disease. With more samples collected, it is possible that even more *Colletotrichum* species, or even novel species, will be characterized as responsible for this disease. Consequently, future attention should be given to probe *Colletotrichum* species collected from *C. paliurus* anthracnose in different geographical areas with different latitudes or elevations in China.

Temperature is an indispensable factor that affects epidemics of anthracnose or other plant diseases (Dubrulle et al., 2020). High temperatures and their frequency may be the factors leading to the delay or non-occurrence of plant diseases (Han et al., 2016; Xue et al., 2019). In the present study, no significant differences occurred in the optimum and minimum mycelial

TABLE 6 | Mean half-maximal effective concentration (EC_{50}) of *Colletotrichum* spp.

Species/ Isolate	EC_{50} (mg/liter)[z]			
	Mycelial growth			Spore germination
	Tetramycin	PCA	Kasugamycin	Tetramycin
C. aenigma				
HC3	2.5 ± 0.01	22.95 ± 6.39	>100	0.02 ± 0.00
SC7	2.59 ± 0.11	42.05 ± 12.64	>100	0.15 ± 0.01
YM8	2.51 ± 0.01	39.5 ± 14.03	>100	0.02 ± 0.01
C. fructicola				
BM5	2.61 ± 0.12	19.54 ± 2.18	>100	0.02 ± 0.01
GX1	2.41 ± 0.08	24.67 ± 4.42	>100	0.02 ± 0.01
HC2	2.65 ± 0.22	24.67 ± 5.3	>100	0.02 ± 0.01
LC7	2.46 ± 0.11	32.24 ± 5.03	>100	0.03 ± 0.02
NC25	2.44 ± 0.01	20.14 ± 0.93	>100	0.01 ± 0.00
SC6	2.45 ± 0.13	26.16 ± 4.85	>100	0.02 ± 0.00
YH6	2.59 ± 0.07	15.61 ± 1.49	>100	0.02 ± 0.00
C. gloeosporioides				
BM6	3.15 ± 0.46	40.71 ± 9.07	>100	0.04 ± 0.01
GX3	2.6 ± 0.19	40.47 ± 9.56	>100	0.02 ± 0.00
LC2	3.1 ± 0.46	40.21 ± 7.54	>100	0.02 ± 0.00
YM4	3.03 ± 0.35	38.03 ± 9.7	>100	0.01 ± 0.00

[z] *Data are mean ± standard error.*

growth temperatures of *C. aenigma* and *C. fructicola*, while *C. gloeosporioides* s. s. isolates exhibited more tolerance to high temperature, which was in concordance with previous study results (Han et al., 2016). These data may provide useful information for *C. paliurus* anthracnose control strategies: fungicide applications should be timed before the optimum growth temperature is reached.

Once infection occurs, the suppression of spore germination and mycelial growth within the plant tissue plays a crucial role in anthracnose management. In the present study, tetramycin showed excellent inhibitory effect on the mycelial growth and spore germination of the three *Colletotrichum* species (**Table 6**). The satisfactory inhibitory activity against different life stages of *Colletotrichum* species indicates that tetramycin may be a potential alternative for the management of *C. paliurus* anthracnose. In previous studies, the excellent curative and protective activity of tetramycin has been widely reported in Phytophthora blight, rice blast, tomato leaf mold, Corynespora leaf spot, and cucumber gray mold (Zhao et al., 2010; Miao et al., 2015; Song et al., 2016; Chen L. L. et al., 2017; Ma et al., 2018a,b), demonstrating that tetramycin would be helpful to prevent the occurrence and spread of plant diseases throughout the field. Accordingly, protective and curative activity of tetramycin on *C. paliurus* anthracnose in the field trials would be further studied before it is put into use.

DATA AVAILABILITY STATEMENT

The datasets presented in this study can be found in online repositories. The names of the repository/repositories and accession number(s) can be found in the article/**Supplementary Material**.

AUTHOR CONTRIBUTIONS

X-RZ was responsible for the entire process of experimentation and writing the manuscript. M-JZ helped perform the experiment and analyze the results. X-LS and S-ZF provided experimental materials. F-MC supervised the work. All authors contributed to manuscript revision and read and approved the submitted version.

FUNDING

This study was financially supported by the Postgraduate Research and Practice Innovation Program of Jiangsu Province (KYCX20_0875).

ACKNOWLEDGMENTS

The authors would like to thank the reviewers for their valuable suggestions on this manuscript.

SUPPLEMENTARY MATERIAL

The Supplementary Material for this article can be found online at: https://www.frontiersin.org/articles/10.3389/fpls.2020.613499/full#supplementary-material

REFERENCES

Alijani, Z., Amini, J., Ashengroph, M., and Bahramnejad, B. (2019). Antifungal activity of volatile compounds produced by *Staphylococcus sciuri* strain MarR44 and its potential for the biocontrol of *Colletotrichum nymphaeae*, causal agent strawberry anthracnose. *Int. J. Food Microbiol.* 307:10827. doi: 10.1016/j.ijfoodmicro.2019.108276

Bautista-Cruz, M. A., Almaguer-Vargas, G., Leyva-Mir, S. G., Colinas-Leon, M. T., Correia, K. C., Camacho-Tapia, M., et al. (2019). Phylogeny, Distribution, and Pathogenicity of *Lasiodiplodia* Species Associated With Cankers and Dieback Symptoms of Persian Lime in Mexico. *Plant Dis.* 103, 1156–1165. doi: 10.1094/PDIS-06-18-1036-RE

Bi, Y., Cui, X., Lu, X., Cai, M., Liu, X., and Hao, J. J. (2011). Baseline Sensitivity of Natural Population and Resistance of Mutants in *Phytophthora capsici* to Zoxamide. *Phytopathology* 101, 1104–1111. doi: 10.1094/PHYTO-01-11-0010

Cai, L., Hyde, K. D., Taylor, P. W. J., Weir, B. S., Waller, J. M., Abang, M. M., et al. (2009). A polyphasic approach for studying *Colletotrichum*. *Fungal Div.* 39, 183–204.

Cannon, P. F., Damm, U., Johnston, P. R., and Weir, B. S. (2012). *Colletotrichum* - current status and future directions. *Stud. Mycol.* 73, 181–213. doi: 10.3114/sim0014

Cao, X. R., Xu, X. M., Che, H. Y., West, J. S., and Luo, D. Q. (2020). Eight *Colletotrichum* species, including a novel species, are associated with areca palm anthracnose in Hainan. *China. Plant Dis.* 104, 1369–1377. doi: 10.1094/PDIS-10-19-2077-RE

Cao, Y., Fang, S., Yin, Z., Fu, X., Shang, X., Yang, W., et al. (2017). Chemical Fingerprint and Multicomponent Quantitative Analysis for the Quality Evaluation of *Cyclocarya paliurus* Leaves by HPLC-Q-TOF-MS. *Molecules* 22:1927. doi: 10.3390/molecules22111927

Carbone, I., and Kohn, L. M. (1999). A method for designing primer sets for speciation studies in filamentous ascomycetes. *Mycologia* 91, 553–556. doi: 10.2307/3761358

Chen, L. L., Guo, B. B., and Li, B. X. (2017). Toxicity and control efficacy of tetramycin against *Passalora fulva*. *Chin. J. Pestic. Sci.* 19, 324–330.

Chen, Y., Qiao, W., Zeng, L., Shen, D., Liu, Z., Wang, X., et al. (2017). Characterization, Pathogenicity, and Phylogenetic Analyses of *Colletotrichum* Species Associated with Brown Blight Disease on *Camellia sinensis* in China. *Plant Dis.* 101, 1022–1028. doi: 10.1094/PDIS-12-16-1824-RE

Damm, U., Cannon, P. F., Woudenberg, J. H. C., and Crous, P. W. (2012). The *Colletotrichum acutatum* species complex. *Stud. Mycol* 73, 37–113. doi: 10.3114/sim0010

Damm, U., Sato, T., Alizadeh, A., Groenewald, J. Z., and Crous, P. W. (2019). The *Colletotrichum dracaenophilum*, *C. magnum and C. orchidearum species complexes*. *Stud. Mycol.* 92, 1–46. doi: 10.1016/j.simyco.2018.04.001

De Silva, D. D., Ades, P. K., Crous, P. W., and Taylor, P. W. J. (2017a). *Colletotrichum* species associated with chili anthracnose in Australia. *Plant Pathol.* 66, 254–267. doi: 10.1111/ppa.12572

De Silva, D. D., Crous, P. W., Ades, P. K., Hyde, K. D., and Taylor, P. W. J. (2017b). Life styles of *Colletotrichum* species and implications for plant biosecurity. *Fungal Biol. Rev.* 31, 155–168. doi: 10.1016/j.fbr.2017.05.001

Dean, R., Van Kan, J. A. L., Pretorius, Z. A., Hammond-Kosack, K. E., Di Pietro, A., Spanu, P. D., et al. (2012). The Top 10 fungal pathogens in molecular plant pathology. *Mol. Plant Pathol.* 13, 804–804. doi: 10.1111/j.1364-3703.2012.00822.x

Deng, B., Cao, Y., Fang, S., Shang, X., Yang, W., and Qian, C. (2015). Variation and stability of growth and leaf flavonoid content in *Cyclocarya paliurus* across environments. *Ind. Crop. Prod.* 76, 386–393. doi: 10.1016/j.indcrop.2015.07.011

Diao, Y. Z., Zhang, C., Liu, F., Wang, W. Z., Liu, L., Cai, L., et al. (2017). *Colletotrichum* species causing anthracnose disease of chili in China. *Persoonia* 38, 20–37. doi: 10.3767/003158517X692788

Duan, Y., Xiao, X., Li, T., Chen, W., Wang, J., Fraaije, B. A., et al. (2018). Impact of epoxiconazole on Fusarium head blight control, grain yield and deoxynivalenol accumulation in wheat. *Pestic. Biochem. Phys.* 152, 138–147. doi: 10.1016/j.pestbp.2018.09.012

Dubrulle, G., Pensec, F., Picot, A., Rigalma, K., Pawtowski, A., Nicolleau, S., et al. (2020). Phylogenetic Diversity and Effect of Temperature on Pathogenicity of *Colletotrichum lupini*. *Plant Dis.* 104, 938–950. doi: 10.1094/PDIS-02-19-0273-RE

Fang, S., Yang, W., Chu, X., Shang, X., She, C., and Fu, X. (2011). Provenance and temporal variations in selected flavonoids in leaves of *Cyclocarya paliurus*. *Food Chem.* 124, 1382–1386. doi: 10.1016/j.foodchem.2010.07.095

Fang, Y., Xia, L., Wang, P., Zhu, L., Ye, J., and Huang, L. (2018). The MAPKKK CgMck1 Is Required for Cell Wall Integrity, Appressorium Development, and Pathogenicity in *Colletotrichum gloeosporioides*. *GENES* 9:543. doi: 10.3390/genes9110543

Freeman, S., Katan, T., and Shabi, E. (1998). Characterization of *Colletotrichum* Species Responsible for Anthracnose Diseases of Various Fruits. *Plant Dis.* 82, 596–605. doi: 10.1094/PDIS.1998.82.6.596

Fu, M., Crous, P. W., Bai, Q., Zhang, P. F., Xiang, J., Guo, Y. S., et al. (2019). Colletotrichum species associated with anthracnose of *Pyrus* spp. *in China*. *Persoonia* 42, 1–35. doi: 10.3767/persoonia.2019.42.01

Gao, Y. Y., Li, X. X., He, L. F., Li, B. X., Mu, W., and Liu, F. (2020). Effect of Pyrisoxazole on *Colletotrichum scovillei* Infection and Anthracnose on Chili. *Plant Dis.* 104, 551–559. doi: 10.1094/PDIS-06-19-1291-RE

Gardes, M., and Bruns, T. D. (1993). ITS primers with enhanced specificity for basidiomycetes–application to the identification of mycorrhizae and rusts. *Mol. Ecol.* 2, 113–118. doi: 10.1111/j.1365-294X.1993.tb00005.x

Glass, N. L., and Donaldson, G. C. (1995). Development of primer sets designed for use with the PCR to amplify conserved genes from filamentous ascomycetes. *Appl. Environ. Microb.* 61, 1323–1330. doi: 10.1128/AEM.61.4.1323-1330.1995

Guarnaccia, V., Groenewald, J. Z., Polizzi, G., and Crous, P. W. (2017). High species diversity in *Colletotrichum* associated with citrus diseases in Europe. *Persoonia* 39, 32–50. doi: 10.3767/persoonia.2017.39.02

Guerber, J. C., Liu, B., Correll, J. C., and Johnston, P. R. (2003). Characterization of diversity in *Colletotrichum acutatum* sensu lato by sequence analysis of two gene introns, mtDNA and intron RFLPs, and mating compatibility. *Mycologia* 95, 872–895. doi: 10.2307/3762016

Gupta, A., Jaiswal, A., and Prachnad, S. (2014). Quantitative structure activity relationship analysis of N-substituted phenazine-1-carboxamides analogs as anti-mycobacterial agents. *Int. J. Pharm. Life Sci.* 5, 3230–3240.

Han, F., Yan, R., Zhang, M., Xiang, Z., Wu, Q., and Li, J. (2020). Synthesis and bioactivities of phenazine-1-carboxylic piperazine derivatives. *Nat. Prod. Res.* 34, 1282–1287. doi: 10.1080/14786419.2018.1556656

Han, Y. C., Zeng, X. G., Xiang, F. Y., Ren, L., Chen, F. Y., and Gu, Y. C. (2016). Distribution and Characteristics of *Colletotrichum* spp. *Associated with Anthracnose of Strawberry in Hubei, China*. *Plant Dis.* 100, 996–1006. doi: 10.1094/PDIS-09-15-1016-RE

He, L. F., Li, X. X., Gao, Y. Y., Li, B. X., Mu, W., and Liu, F. (2019). Characterization and Fungicide Sensitivity of *Colletotrichum* spp. *from Different Hosts in Shandong, China*. *Plant Dis.* 103, 34–43. doi: 10.1094/PDIS-04-18-0597-RE

Hu, M., Grabke, A., Dowling, M. E., Holstein, H. J., and Schnabel, G. (2015). Resistance in *Colletotrichum siamense* From Peach and Blueberry to Thiophanate-Methyl and Azoxystrobin. *Plant Dis.* 99, 806–814. doi: 10.1094/PDIS-10-14-1077-RE

Huang, L., Li, Q., Zhang, Y., Li, D., and Ye, J. (2016). *Colletotrichum gloeosporioides* sensu stricto Is a Pathogen of Leaf Anthracnose on Evergreen Spindle Tree (*Euonymus japonicus*). *Plant Dis.* 100, 672–678. doi: 10.1094/PDIS-07-15-0740-RE

Huang, L., Zhu, Y., Yang, J., Li, D., Li, Y., Bian, L., et al. (2018). Shoot Blight on Chinese Fir (*Cunninghamia lanceolate*) is Caused by *Bipolaris oryzae*. *Plant Dis.* 102, 500–506. doi: 10.1094/PDIS-07-17-1032-RE

Hyde, K. D., Cai, L., Cannon, P. F., Crouch, J. A., Crous, P. W., Damm, U., et al. (2009). *Colletotrichum* - names in current use. *Fungal Div.* 39, 147–182.

Jayawardena, R. S., Huang, J., Jin, B., Yan, J., Li, X., Hyde, K., et al. (2016). An account of *Colletotrichum* species associated with strawberry anthracnose in China based on morphology and molecular data. *Mycosphere* 7, 1147–1163. doi: 10.5943/mycosphere/si/2c/6

Kim, H., Lee, K., and Chae, J. (2015). Postharvest Biological Control of *Colletotrichum acutatum* on Apple by *Bacillus subtilis* HM1 and the Structural Identification of Antagonists. *J. Microbiol. Biotechn.* 25, 1954–1959. doi: 10.4014/jmb.1507.07100

Konsue, W., Dethoup, T., and Limtong, S. (2020). Biological Control of Fruit Rot and Anthracnose of Postharvest Mango by Antagonistic Yeasts from Economic Crops Leaves. *Microorganisms* 8:317. doi: 10.3390/microorganisms8030317

Kumar, S., Stecher, G., and Tamura, K. (2016). MEGA7: Molecular Evolutionary Genetics Analysis Version 7.0 *for Bigger Datasets*. *Mol. Biol. Evol.* 33, 1870–1874. doi: 10.1093/molbev/msw054

Liu, F., Cai, L., Crous, P. W., and Damm, U. (2014). The *Colletotrichum gigasporum* species complex. *Persoonia* 33, 83–97. doi: 10.3767/003158514X684447

Liu, F., Wang, M., Damm, U., Crous, P. W., and Cai, L. (2016). Species boundaries in plant pathogenic fungi: a *Colletotrichum* case study. *BMC Evol. Biol.* 16:81. doi: 10.1186/s12862-016-0649-5

Liu, F., Weir, B. S., Damm, U., Crous, P. W., Wang, Y., Liu, B., et al. (2015). Unravelling *Colletotrichum* species associated with Camellia: employing ApMat and GS loci to resolve species in the *C. gloeosporioides complex*. *Persoonia* 35, 63–86. doi: 10.3767/003158515X687597

Liu, Y., Chen, P., Zhou, M., Wang, T., Fang, S., Shang, X., et al. (2018a). Geographic Variation in the Chemical Composition and Antioxidant Properties of Phenolic Compounds from *Cyclocarya paliurus* (Batal) Iljinskaja Leaves. *Molecules* 23:2440. doi: 10.3390/molecules23102440

Liu, Y., Fang, S., Zhou, M., Shang, X., Yang, W., and Fu, X. (2018b). Geographic variation in water-soluble polysaccharide content and antioxidant activities of *Cyclocarya paliurus* leaves. *Ind. Crop. Prod.* 121, 180–186. doi: 10.1016/j.indcrop.2018.05.017

Logua, A. D., Palchykovska, L. H., Kostina, V. H., Sanna, A., Meleddu, R., Chisu, L., et al. (2009). Novel N-aryl- and N-heteryl-phenazine-1-carboxamides as potential agents for the treatment of infections sustained by drug-resistant and MDR Mycobacterium tuberculosis. *Int. J. Antimicrob. Ag.* 33, 223–229. doi: 10.1016/j.ijantimicag.2008.09.016

Lu, X. H., Zhu, S. S., Bi, Y., Liu, X. L., and Hao, J. J. (2010). Baseline Sensitivity and Resistance-Risk Assessment of *Phytophthora capsici* to Iprovalicarb. *Phytopathology* 100, 1162–1168. doi: 10.1094/PHYTO-12-09-0351

Ma, D., Zhu, J., He, L., Cui, K., Mu, W., and Liu, F. (2018a). Baseline Sensitivity and Control Efficacy of Tetramycin Against *Phytophthora capsici* Isolates in China. *Plant Dis.* 102, 863–868. doi: 10.1094/PDIS-09-17-1396-RE

Ma, D., Zhu, J., Jiang, J., Zhao, Y., Li, B., Mu, W., et al. (2018b). Evaluation of bioactivity and control efficacy of tetramycin against *Corynespora cassiicola*. *Pestic. Biochem. Phys.* 152, 106–113. doi: 10.1016/j.pestbp.2018.09.009

Manire, C. A., Rhinehart, H. L., Sutton, D. A., Thompson, E. H., Rinaldi, M. G., Buck, J. D., et al. (2002). Disseminated mycotic infection caused by *Colletotrichum acutatum* in a Kemp's ridley sea turtle (*Lepidochelys kempi*). *J. Clin. Microbiol.* 40, 4273–4280. doi: 10.1128/JCM.40.11.4273-4280.2002

McGhee, G. C., and Sundin, G. W. (2011). Evaluation of kasugamycin for fire blight management, effect on nontarget bacteria, and assessment of kasugamycin resistance potential in *Erwinia amylovora*. *Phytopathology* 101, 192–204. doi: 10.1094/PHYTO-04-10-0128

Miao, J., Dong, X., and Lin, D. (2015). Activity of the novel fungicide oxathiapiprolin against plant-pathogenic oomycetes. *Pest Manage. Sci.* 72, 1572–1577. doi: 10.1002/ps.4189

Mo, J., Zhao, G., Li, Q., Solangi, G. S., Tang, L., Guo, T., et al. (2018). Identification and characterization of *Colletotrichum* species associated with mango anthracnose in Guangxi. *China*. *Plant Dis.* 102, 1283–1289. doi: 10.1094/PDIS-09-17-1516-RE

Moreira, R. R., and May De Mio, L. L. (2015). Potential biological agents isolated from apple fail to control Glomerella leaf spot in the field. *Biol. Control* 87, 56–63. doi: 10.1016/j.biocontrol.2015.04.020

Munir, M., Amsden, B., Dixon, E., Vaillancourt, L., and Gauthier, N. A. W. (2016). Characterization of *Colletotrichum* Species Causing Bitter Rot of Apple

in Kentucky Orchards. *Plant Dis.* 100, 2194–2203. doi: 10.1094/PDIS-10-15-1144-RE

O'Donnell, K., Nirenberg, H. I., Aoki, T., and Cigelnik, E. (2000). A Multigene phylogeny of the *Gibberella fujikuroi* species complex: Detection of additional phylogenetically distinct species. *Mycoscience* 41, 61–78. doi: 10.1007/BF02464387

O'Connell, R. J., Thon, M. R., Hacquard, S., Amyotte, S. G., Kleemann, J., Torres, M. F., et al. (2012). Lifestyle transitions in plant pathogenic *Colletotrichum* fungi deciphered by genome and transcriptome analyses. *Nat. Genet.* 44, 1060–1065. doi: 10.1038/ng.2372

O'Donnell, K., and Cigelnik, E. (1997). Two divergent intragenomic rDNA ITS2 types within a monophyletic lineage of the fungus *Fusarium* are nonorthologous. *Mol. Phylogenet. Evol.* 7, 103–116. doi: 10.1006/mpev.1996.0376

Palchykovska, L. G., Vasylchenko, O. V., Platonov, M. O., Kostina, V. G., Babkina, M. M., Tarasov, O. A., et al. (2012). Evaluation of antibacterial and antiviral activity of N-arylamides of 9-methyl and 9-methoxyphenazine-1-carboxylic acids -inhibitors of the phage T7 model transctiption. *Biopolym. Cell* 28, 477–485. doi: 10.7124/bc.00013A

Prihastuti, H., Cai, L., Chen, H., McKenzie, E. H. C., and Hyde, K. D. (2009). Characterisation of *Colletotrichum* species associated with coffee berries in northern Thailand. *Fungal Div.* 39, 89–109.

Ren, J., Cui, Y., Zhang, F., Cui, H., Ni, X., Chen, F., et al. (2014). Enhancement of nystatin production by redirecting precursor fluxes after disruption of the tetramycin gene from *Streptomyces ahygroscopicus*. *Microbiol. Res.* 169, 602–608. doi: 10.1016/j.micres.2013.09.017

Ronquist, F., Teslenko, M., van der Mark, P., Ayres, D. L., Darling, A., Hohna, S., et al. (2012). MrBayes 3.2*: Efficient Bayesian Phylogenetic Inference and Model Choice Across a Large Model Space*. *Syst. Biol.* 61, 539–542. doi: 10.1093/sysbio/sys029

Sangeetha, C. G., and Rawal, R. D. (2008). Nutritional studies of *Colletotrichum gloeosporioides* (Penz.) *Penz. and Sacc. the incitant of mango anthracnose*. *World J. Agric. Sci.* 4, 717–720.

Sharma, G., Maymon, M., and Freeman, S. (2017). Epidemiology, pathology and identification of *Colletotrichum* including a novel species associated with avocado (*Persea americana*) anthracnose in Israel. *Sci. Rep.* 7:15839. doi: 10.1038/s41598-017-15946-w

Silva, D. N., Talhinhas, P., Várzea, V., Cai, L., Paulo, O. S., and Batista, D. (2012). Application of the Apn2/MAT locus to improve the systematics of the *Colletotrichum gloeosporioides* complex: an example from coffee (*Coffea* spp.) *hosts*. *Mycologia* 104, 396–409. doi: 10.3852/11-145

Simionato, A. S., Navarro, M. O. P., de Jesus, M. L. A., Barazetti, A. R., Da Silva, C. S., Simoes, G. C., et al. (2017). The Effect of Phenazine-1-Carboxylic Acid on Mycelial Growth of *Botrytis cinerea* Produced by *Pseudomonas aeruginosa* LV Strain. *Front. Microbiol.* 8:1102. doi: 10.3389/fmicb.2017.01102

Song, Y., He, L., Chen, L., Ren, Y., Lu, H., Geng, S., et al. (2016). Baseline sensitivity and control efficacy of antibiosis fungicide tetramycin against *Botrytis cinerea*. *Eur. J. Plant Pathol.* 146, 337–347. doi: 10.1007/s10658-016-0920-z

Than, P. P., Jeewon, R., Hyde, K. D., Pongsupasamit, S., Mongkolporn, O., and Taylor, P. W. J. (2008). Characterization and pathogenicity of *Colletotrichum* species associated with anthracnose on chilli (*Capsicum* spp.) *in Thailand*. *Plant Pathol.* 57, 562–572. doi: 10.1111/j.1365-3059.2007.01782.x

Udayanga, D., Manamgoda, D. S., Liu, X. Z., Chukeatirote, E., and Hyde, K. D. (2013). What are the common anthracnose pathogens of tropical fruits? *Fungal Diver.* 61, 165–179. doi: 10.1007/s13225-013-0257-2

Udumula, V., Endres, J. L., Harper, C. N., Jaramillo, L., Zhong, H. A., Bayles, K. W., et al. (2017). Simple synthesis of endophenazine G and other phenazines and their evaluation as anti-methicillin-resistant *Staphylococcus aureus* agents. *Eur. J. Med. Chem.* 125, 710–721. doi: 10.1016/j.ejmech.2016.09.079

Uppala, S., and Zhou, X. G. (2018). Field efficacy of fungicides for management of sheath blight and narrow brown leaf spot of rice. *Crop Prot.* 104, 72–77. doi: 10.1016/j.cropro.2017.10.017

Vieira, W. A. D., Bezerra, P. A., da Silva, A. C., Veloso, J. S., Camara, M. P. S., Doyle, V. P., et al. (2020). Optimal markers for the identification of *Colletotrichum* species. *Mol. Phylogenet. Evol.* 143:106694. doi: 10.1016/j.ympev.2019.106694

Wang, Q. H., Fan, K., Li, D. W., Han, C. M., Qu, Y. Y., Qi, Y. K., et al. (2020). Identification, Virulence and Fungicide Sensitivity of *Colletotrichum gloeosporioides* s.s. *Responsible for Walnut Anthracnose Disease in China*. *Plant Dis.* 104, 1358–1368. doi: 10.1094/PDIS-12-19-2569-RE

Wang, Q., Jiang, C., Fang, S., Wang, J., Ji, Y., Shang, X., et al. (2013). Antihyperglycemic, antihyperlipidemic and antioxidant effects of ethanol and aqueous extracts of *Cyclocarya paliurus* leaves in type 2 diabetic rats. *J. Ethnopharmacol.* 150, 1119–1127. doi: 10.1016/j.jep.2013.10.040

Weir, B. S., Johnston, P. R., and Damm, U. (2012). The *Colletotrichum gloeosporioides* species complex. *Stud. Mycol.* 73, 115–180. doi: 10.3114/sim0011

White, T. J., Bruns, T., Lee, S., and Taylor, J. W. (1990). *Amplification and direct sequencing of fungal ribosomal RNA genes for phylogenetics. In: PCR Protocols: A Guide to Methods and Applications*. New York: Academic Press

Wikee, S., Cai, L., Pairin, N., McKenzie, E. H. C., Su, Y., Chukeatirote, E., et al. (2011). *Colletotrichum* species from Jasmine (*Jasminum sambac*). *Fungal Div.* 46, 171–182. doi: 10.1007/s13225-010-0049-x

Xie, J., Dong, C., Nie, S., Li, F., Wang, Z., Shen, M., et al. (2015). Extraction, chemical composition and antioxidant activity of flavonoids from *Cyclocarya paliurus* (Batal.) *Iljinskaja leaves*. *Food Chem.* 186, 97–105. doi: 10.1016/j.foodchem.2014.06.106

Xie, J., Liu, X., Shen, M., Nie, S., Zhang, H., Li, C., et al. (2013). Purification, physicochemical characterisation and anticancer activity of a polysaccharide from *Cyclocarya paliurus* leaves. *Food Chem.* 136, 1453–1460. doi: 10.1016/j.foodchem.2012.09.078

Xie, J., Wang, W., Dong, C., Huang, L., Wang, H., Li, C., et al. (2018). Protective effect of flavonoids from *Cyclocarya paliurus* leaves against carbon tetrachloride-induced acute liver injury in mice. *Food Chem. Toxicol.* 119, 392–399. doi: 10.1016/j.fct.2018.01.016

Xie, J., Xie, M., Nie, S., Shen, M., Wang, Y., and Li, C. (2010). Isolation, chemical composition and antioxidant activities of a water-soluble polysaccharide from *Cyclocarya paliurus* (Batal.) *Iljinskaja*. *Food Chem.* 119, 1626–1632. doi: 10.1016/j.foodchem.2009.09.055

Xie, M. Y., Li, L., Nie, S. P., Wang, X. R., and Lee, F. (2006). Determination of speciation of elements related to blood sugar in bioactive extracts from *Cyclocarya paliurus* leaves by FIA-ICP-MS. *Eur. Food Res. Technol.* 223, 202–209. doi: 10.1007/s00217-005-0173-0

Xue, L., Zhang, L., Yang, X. X., Huang, X., Wu, W., Zhou, X., et al. (2019). Characterization, Phylogenetic Analyses, and Pathogenicity of *Colletotrichum* Species on *Morus alba* in Sichuan Provine, China. *Plant Dis.* 103, 2624–2633. doi: 10.1094/PDIS-06-18-0938-RE

Zhang, J., Huang, N., Lu, J., Li, X., Wang, Y., Yang, L., et al. (2010). Water-soluble Phenolic Compounds and Their Anti-HIV-1 Activities from the Leaves of *Cyclocarya paliurus*. *J. Food Drug Anal.* 18, 398–404.

Zhao, X. H., Zhong, L. J., and Zhang, Q. H. (2010). Effect of tetramycin on mycelial growth and spore germination of rice blast pathogen. *J. Microbiol.* 30, 43–45.

Zheng, X., Zhang, M., Shang, X., Fang, S., and Chen, F. (2020). Stem Canker on *Cyclocarya paliurus* Is Caused by *Botryosphaeria dothidea*. *Plant Dis.* 104, 1032–1040. doi: 10.1094/PDIS-11-18-1990-RE

Zhong, L. J., Zhao, X. H., Zhang, Q. H., Xu, C., and Zhu, H. L. (2010). Rice resistance against blast induced by tetramycin. *Plant Dis. Pests* 1, 6–8.

Zhu, X., Yu, L. H., Hsiang, T., Huang, D., Xu, Z. H., Wu, Q. L., et al. (2019). The influence of steric configuration of phenazine-1-carboxylic acid-amino acid conjugates on fungicidal activity and systemicity. *Pest Manag. Sci.* 75, 3323–3330. doi: 10.1002/ps.5455

Zhu, X., Yu, L., Zhang, M., Xu, Z., Yao, Z., Wu, Q., et al. (2018). Design, synthesis and biological activity of hydroxybenzoic acid ester conjugates of phenazine-1-carboxylic acid. *Chem. Cent. J.* 12, 1–10. doi: 10.1186/s13065-018-0478-2

Conflict of Interest: The authors declare that the research was conducted in the absence of any commercial or financial relationships that could be construed as a potential conflict of interest.